UNIVERSIDAD DE CONCEPCIÓN

Centro de Investigación en Ingeniería Matemática (CI^{2}MA)

Numerical analysis of a stabilized mixed method applied to incompressible elasticity problems with Dirichlet and with mixed boundary conditions

Tomás Barrios, Edwin Behrens,
Rommel Bustinza

PREPRINT 2021-26

SERIE DE PRE-PUBLICACIONES

Numerical analysis of a stabilized mixed method applied to incompressible elasticity problems with Dirichlet and with mixed boundary conditions

Tomás P. Barrios [*], Edwin M. Behrens [†] and Rommel Bustinza [‡]

Abstract

We analyze a new stabilized dual-mixed method applied to incompressible linear elasticity problems, considering two kind of data on the boundary of the domain: nonhomogeneous Dirichlet and mixed boundary conditions. In this approach, we circumvent the standard use of the rotation to impose weakly the symmetry of stress tensor. We prove that the new variational formulation and the corresponding Galerkin scheme are well-posed. We also provide the rate of convergence when each row of the stress is approximated by Raviart-Thomas elements and the displacement is approximated by continuous piecewise polynomials. Moreover, we derive a residual a posteriori error estimator for each situation. The corresponding analysis is quite different, depending on the type of boundary conditions. For known displacement on the whole boundary, we based our analysis on Ritz projection of the error, and requires a suitable quasi-Helmholtz decomposition of functions living in $H(\mathbf{div};\Omega)$. As a result, we obtain a simple a posteriori error estimator, that consists of five residual terms, and results to be reliable and locally efficient. On the other hand, when we consider mixed boundary conditions, these tools are not necessary. Then, we are able to develop an a posteriori error analysis, which provide us of an estimator consisting of three residual terms. In addition, we prove that in general this estimator is reliable, and when the traction datum is piecewise polynomial, locally efficient. In the second situation, we propose a numerical procedure to compute the numerical approximation, at a reasonable cost. Finally, we include several numerical experiments that illustrate the performance of the corresponding adaptive algorithm for each problem, and support its use in practice.

Mathematics Subject Classifications (1991): 65N15, 65N30, 65N50

Key words: A posteriori error estimates, augmented mixed formulation, Ritz projection of the error, quasi-Helmholtz decomposition.

[*]Departamento de Matemática y Física Aplicadas, Universidad Católica de la Santísima Concepción, Alonso de Ribera 2850, Concepción (Chile). E-mail: `tomas@ucsc.cl`

[†]Departamento de Ingeniería Civil, Universidad Católica de la Santísima Concepción, Alonso de Ribera 2850, Concepción (Chile). E-mail: `ebehrens@ucsc.cl`

[‡]Departamento de Ingeniería Matemáticas, Universidad de Concepción, Casilla 160-C, Concepción (Chile). E-mail: `rbustinz@ing-mat.udec.cl`.

1 Introduction

In this paper, we are concerned with the development of efficient numerical methods for linear elasticity equations by using a stabilized Galerkin finite element method. Let $\Omega \subset \mathbb{R}^2$ be a bounded and simply connected domain with a Lipschitz-continuous boundary $\Gamma := \partial\Omega$ of an elastic body subject to an exterior force $\boldsymbol{f} \in [L^2(\Omega)]^2$ and a given displacement boundary condition $\boldsymbol{g}$. The kinematic model of linear elasticity seeks a displacement vector field $\boldsymbol{u}$ satisfying

$$-\mathbf{div}(\boldsymbol{\sigma}(\boldsymbol{u})) = \boldsymbol{f} \quad \text{in} \quad \Omega\,, \quad \boldsymbol{u} = \boldsymbol{g} \quad \text{on} \quad \Gamma\,,$$

where $\boldsymbol{\sigma}(\boldsymbol{u})$ is the symmetric Cauchy stress tensor. For linear, homogeneous, and isotropic materials, the Cauchy stress tensor is given by

$$\boldsymbol{\sigma}(\boldsymbol{u}) = 2\,\mu\,\boldsymbol{\varepsilon}(\boldsymbol{u}) + \lambda\,\mathrm{div}(\boldsymbol{u})\,\boldsymbol{I}\,,$$

where $\boldsymbol{\varepsilon}(\boldsymbol{u}) := \frac{1}{2}\left(\nabla\boldsymbol{u} + (\nabla\boldsymbol{u})^{\mathtt{t}}\right)$ is the strain tensor, $\boldsymbol{I}$ represents the identity tensor of order 2, μ and λ are the Lamé constants, which are given by

$$\lambda = \frac{E\nu}{(1+\nu)(1-2\nu)}, \quad \mu, = \frac{E}{2(1+\nu)}\,,$$

with $E > 0$ being the elasticity modulus and $\nu \in (0, 1/2)$ represents the Poisson's ratio. Usually, locking refers to a phenomenon of numerical approximations for a certain problems whose mathematical formulations involve a parameter dependency. For the linear elasticity problem, the parameter is the Poisson ratio ν. For ν close to $1/2$ (i.e., when the material is called nearly incompressible), the parameter λ tends to infinite, furthermore in the limit case $\nu = 1/2$ (or $\lambda = +\infty$) the exact solution presupposes the existence of a finite hydrostatic pressure $p = \lambda\,\mathrm{div}(\boldsymbol{u})$ in Ω, then when λ is infinite, the condition of incompressibility is obtained since the displacement must satisfy the constraint $\mathrm{div}(\boldsymbol{u}) = 0$ in Ω.

In this way, a formulation of the elasticity problem that is able to represent the incompressible behaviour, can be written considering the hydrostatic pressure p as an independent unknown, additional to the displacement field $\boldsymbol{u}$. Therefore, we consider the problem: *Find the displacement $\boldsymbol{u}$, the hydrostatic pressure p and the stress tensor $\boldsymbol{\sigma}$ of a linear incompressible elastic material occupying the region Ω such that*

$$\begin{cases} \boldsymbol{\sigma} = 2\,\mu\,\boldsymbol{\varepsilon}(\boldsymbol{u}) + p\,\boldsymbol{I} & \text{in}\,\Omega\,, \\ -\mathbf{div}(\boldsymbol{\sigma}) = \boldsymbol{f} & \text{in}\,\Omega\,, \\ \mathrm{div}(\boldsymbol{u}) = 0 & \text{in}\,\Omega\,, \\ \boldsymbol{u} = \boldsymbol{g} & \text{on}\,\Gamma\,, \end{cases} \tag{1}$$

where for uniqueness purpose, we seek $p \in L^2_0(\Omega) := \{q \in L^2(\Omega) : \int_\Omega q = 0\}$. In addition, $\boldsymbol{g}$ must satisfy the compatibility condition: $\int_\Gamma \boldsymbol{g}\cdot\boldsymbol{\nu} = 0$, with $\boldsymbol{\nu}$ being the unit outward normal vector to Γ. We remark that problem (1) has already been analyzed in [23], introducing the so-called displacement-pressure formulation, i.e., eliminating the stress. Here, we study the dual mixed formulation which, as it is very well known, allows us to improve the approximation of the stress. A similar structure to the equations described in (1) can be found in [29], where an augmented mixed finite element method for the incompressible fluid flow was introduced. The approach there follows the ideas developed in [31] for the linear elasticity problem, i.e., the incompressible fluid flow is formulated using a dual mixed method and the resulting variational formulation is stabilized in order to deduce a strongly coercive bilinear form. As consequence, the simplest choice of stable finite element subspaces (cf. [29]) is Raviart-Thomas spaces of lowest order for the stress tensor, piecewise linear elements for the displacement, and piecewise constants for the rotation. However, following the ideas developed in [20] for the augmented mixed method, it is possible to eliminate the rotation and thus to reduce the degrees of freedom for the discrete scheme. In this way, our first interest in this article is to explore the use of augmented mixed method to approximate the solution of (1), circumventing the use of the rotation. Secondly, we plan to extend the application of the approach to the case when we deal with Dirichlet and traction data on different parts of the boundary of the domain.

On the other hand, nowadays it is well established that one should apply adaptive mesh refinement based on a posteriori error estimators for efficient implementation of numerical methods. Various types of error estimators have been developed and successfully implemented for the linear elasticity problem; see, for example, the survey papers [37] and [21]. We are particularly interested in the error estimators developed for augmented mixed approach of low computational cost. More specifically, concerning linear elasticity problem, in [7] we present an alternative a posteriori error estimator to the ones developed in [17]. This approach is based on the Ritz projection of the error (see [16]), and in the case of homogeneous Dirichlet boundary condition, we obtain a reliable and local efficient a posteriori error estimator, that only requires the computation of five residuals per element at most, which is a low computational cost comparing with the eleven terms included in the estimator developed in [17] for the same case. Furthermore, a similar reduction we have deduced for the extension to elasticity problem with non homogeneous Dirichlet and mixed boundary conditions whose a posteriori error analysis is presented in [6] and the corresponding low cost estimators were introduced in [7] and [9], respectively. Additionally, we comment that this kind of a posteriori error estimator, at least, have been developed successfully in other applications. For example, in fluid mechanics framework we can mention the study of the Darcy flow in [13] and [14], the Brinkman model in [11] and [10], a general pseudo-compressible and incompressible fluid flow in [4] and [8], respectively, and the Oseen equations in [15]. Then, our second aim in this article is to develop the corresponding a posteriori estimator of low computational cost, for each one of the boundary value problems, in order to obtain an efficient implementation for the new approaches. We remark that the analysis we present in this work, is valid for 2D and 3D cases. For simplicity, we will describe it for 2D case.

The rest of the paper is organized as follows. In Section 2, with the purpose of clarifying the presentation, we deduce the dual mixed variational formulation for the incompressible elasticity in the plane. A stabilization mechanism for this formulation is introduced in Section 3, as well as the Galerkin scheme and the simplest finite element subspaces that can be used. In Section 4, we develop the a posteriori error analysis and propose the new a posteriori error estimate. The extension to mixed boundary conditions is established in Section 5, while in Section 6 we derive a corresponding a posteriori error estimator. Finally, in Section 7 we provide several numerical experiments that support the use of the theoretical results in practice.

We end this section with some notations to be used throughout the paper. Given a Hilbert space H, we denote by H^2 (resp., $H^{2\times 2}$) the space of vectors (resp., square tensors) of order 2 with entries in H. Given $\boldsymbol{\tau} := (\tau_{ij})$ and $\boldsymbol{\zeta} := (\zeta_{ij}) \in \mathbb{R}^{2\times 2}$, we denote $\boldsymbol{\tau}^{\mathtt{t}} := (\tau_{ji})$, $\mathrm{tr}(\boldsymbol{\tau}) := \tau_{11} + \tau_{22}$, $\boldsymbol{\tau}^{\mathtt{d}} := \boldsymbol{\tau} - \frac{1}{2}\mathrm{tr}(\boldsymbol{\tau})\,\boldsymbol{I}$ and $\boldsymbol{\tau} : \boldsymbol{\zeta} := \sum_{i,j=1}^{2} \tau_{ij}\,\zeta_{ij}$. We also use the standard notations for Sobolev spaces and norms. We denote by $H(\mathbf{div};\Omega) := \{\boldsymbol{\tau} \in [L^2(\Omega)]^{2\times 2} : \mathbf{div}(\boldsymbol{\tau}) \in [L^2(\Omega)]^2\}$, $H_0(\mathbf{div};\Omega) := \{\boldsymbol{\tau} \in H(\mathbf{div};\Omega) : \int_\Omega \mathrm{tr}(\boldsymbol{\tau}) = 0\}$. We recall that $H(\mathbf{div};\Omega) = H_0(\mathbf{div};\Omega) \oplus \mathbb{R}\,\boldsymbol{I}$, that is, for any $\boldsymbol{\tau} \in H(\mathbf{div};\Omega)$ there exists a unique $\boldsymbol{\tau}_0 \in H_0(\mathbf{div};\Omega)$ and $\lambda := \frac{1}{2|\Omega|}\int_\Omega \mathrm{tr}(\boldsymbol{\tau}) \in \mathbb{R}$ such that $\boldsymbol{\tau} = \boldsymbol{\tau}_0 + \lambda\,\boldsymbol{I}$. Finally, C or c (with or without subscripts) will denote generic constants, independent of the discretization parameters, that may take different values at different occurrences.

2 The dual-mixed formulation

In this section, we describe the classical technique to impose weakly the symmetry of the stress tensor developed in the early work [1] (also, see [31]). This relies on the introduction of an additional unknown, called the rotation $\boldsymbol{\gamma} := \frac{1}{2}(\nabla\boldsymbol{u} - (\nabla\boldsymbol{u})^{\mathtt{t}}) \in [L^2(\Omega)]^{2\times 2}_{\mathtt{skew}} := \{\boldsymbol{\eta} \in [L^2(\Omega)]^{2\times 2} : \boldsymbol{\eta} + \boldsymbol{\eta}^{\mathtt{t}} = \mathbf{0}\}$. As a result, we have $\boldsymbol{\varepsilon}(\boldsymbol{u}) = \nabla\boldsymbol{u} - \boldsymbol{\gamma}$ in Ω. This allows us to rewrite the first equation in (1) as

$$\frac{1}{2\,\mu}\,\boldsymbol{\sigma} \,=\, \nabla\boldsymbol{u} \,-\, \boldsymbol{\gamma} \,+\, \frac{1}{2\,\mu}\,p\,\boldsymbol{I} \quad \text{in } \Omega\,. \tag{2}$$

Noticing that $\mathrm{tr}(\boldsymbol{\sigma}) = 2\,p$ in Ω, we deduce that $\boldsymbol{\sigma} \in H_0(\mathbf{div};\Omega)$. Then, we can eliminate the pressure p from (2), to derive

$$\frac{1}{2\,\mu}\,\boldsymbol{\sigma}^{\mathtt{d}} \,=\, \nabla\boldsymbol{u} \,-\, \boldsymbol{\gamma} \quad \text{in } \Omega\,. \tag{3}$$

Next, proceeding in standard way, we deduce the following variational formulation of (1): *Find* $(\boldsymbol{\sigma}, \boldsymbol{u}, \boldsymbol{\gamma}) \in H_0(\mathbf{div};\Omega) \times [L^2(\Omega)]^2 \times [L^2(\Omega)]^{2\times 2}_{\mathtt{skew}}$ *such that*

$$\frac{1}{2\,\mu}\int_\Omega \boldsymbol{\sigma}^{\mathtt{d}} : \boldsymbol{\tau}^{\mathtt{d}} + \int_\Omega \boldsymbol{u}\cdot\mathbf{div}(\boldsymbol{\tau}) + \int_\Omega \boldsymbol{\gamma} : \boldsymbol{\tau} = \langle \boldsymbol{\tau\nu}, \boldsymbol{g}\rangle_\Gamma \qquad \forall\boldsymbol{\tau} \in H_0(\mathbf{div};\Omega)\,, \tag{4}$$

$$-\int_\Omega \boldsymbol{v}\cdot\mathbf{div}(\boldsymbol{\sigma}) - \int_\Omega \boldsymbol{\eta} : \boldsymbol{\sigma} = \int_\Omega \boldsymbol{f}\cdot\boldsymbol{v} \qquad \forall(\boldsymbol{v},\boldsymbol{\eta}) \in [L^2(\Omega)]^2 \times [L^2(\Omega)]^{2\times 2}_{\mathtt{skew}}\,. \tag{5}$$

Hereafter, by $\langle\cdot,\cdot\rangle_\Gamma$ we denote the duality pairing of $H^{-1/2}(\Gamma)$ and $H^{1/2}(\Gamma)$ with respect to the $L^2(\Gamma)$ inner product.

In order to prove the unique solvability of the variational formulation, we rewrite it now as a system of operator equations with a saddle point structure. To this end, we first define the spaces $X := H_0(\mathbf{div};\Omega)$, $M := [L^2(\Omega)]^2 \times [L^2(\Omega)]^{2\times 2}_{\mathtt{skew}}$. Then, we introduce the operators and functionals $\boldsymbol{A} : X \to X'$, $\boldsymbol{B} : X \to M'$, $\boldsymbol{S} : M \to M'$, $G \in X'$, and $F \in M'$, as suggested by the structure of (4)-(5), so that this problem can be stated as: Find $(\boldsymbol{\sigma}, (\boldsymbol{u}, \boldsymbol{\gamma})) \in X \times M$ such that

$$\begin{cases} [\boldsymbol{A}(\boldsymbol{\sigma}), \boldsymbol{\tau}] + [\boldsymbol{B}(\boldsymbol{\tau}), (\boldsymbol{u}, \boldsymbol{\gamma})] & = [G, \boldsymbol{\tau}] \quad \forall\,\boldsymbol{\tau} \in X\,, \\ [\boldsymbol{B}(\boldsymbol{\sigma}), (\boldsymbol{v}, \boldsymbol{\eta})] & = [F, (\boldsymbol{v}, \boldsymbol{\eta})] \quad \forall\,(\boldsymbol{v}, \boldsymbol{\eta}) \in M\,, \end{cases} \tag{6}$$

where $[\cdot,\cdot]$ denotes the duality pairing induced by operators and functionals used in each case. We recall now an important result that will help us to prove the unique solvability of (6).

Lemma 1 *There exists $c_1 > 0$, depending only on Ω, such that*

$$\forall\, \boldsymbol{\tau} \in H_0(\mathbf{div};\Omega) \,:\, c_1\, \|\boldsymbol{\tau}\|^2_{[L^2(\Omega)]^{2\times 2}} \,\leq\, \|\boldsymbol{\tau}^{\mathtt{d}}\|^2_{[L^2(\Omega)]^{2\times 2}} + \|\mathbf{div}(\boldsymbol{\tau})\|^2_{[L^2(\Omega)]^2}\,. \tag{7}$$

Proof. We refer to Proposition 3.1 of Chapter IV in [19], or Lemma 3.1 in [2]. □

Existence and uniqueness of the solution of (6) are established in the next result.

Theorem 2 *Problem* (6) *has a unique solution $(\boldsymbol{\sigma},(\boldsymbol{u},\boldsymbol{\gamma})) \in X \times M$. Moreover, there exists a positive constant C, independent of the solution, such that*

$$||(\boldsymbol{\sigma},(\boldsymbol{u},\boldsymbol{\gamma}))||_{X\times M} \leq C\,(\,||F||_{X'} \,+\, ||G||_{M'}\,)\,.$$

Proof. First, we notice that the operators $\boldsymbol{A}$, $\boldsymbol{B}$, as well as the functionals F and G, are all linear and bounded. In addition, it is not difficult to deduce

$$N(\boldsymbol{B}) := \text{Kernel}(\boldsymbol{B}) := \{\boldsymbol{\tau} \in X \;:\quad \boldsymbol{\tau} = \boldsymbol{\tau}^{\mathtt{t}} \quad \text{in} \quad \Omega \quad \text{and} \quad \mathbf{div}(\boldsymbol{\tau}) \,=\, \mathbf{0} \quad \text{in} \quad \Omega\}.$$

Now, invoking (7), we have for any $\boldsymbol{\tau} \,\in\, N(\boldsymbol{B})$

$$[\boldsymbol{A}(\boldsymbol{\tau}),\boldsymbol{\tau}] \,=\, \frac{1}{2\,\mu}\,\|\boldsymbol{\tau}^{\mathtt{d}}\|^2_{[L^2(\Omega)]^{2\times 2}} \,\geq\, \frac{c_1}{2\,\mu}\,\|\boldsymbol{\tau}\|^2_X\,,$$

and therefore we ensure the coercivity of $\boldsymbol{A}$ on $N(\boldsymbol{B})$. In addition, thanks to Lemma 4.3 in [3], $\boldsymbol{B}$ satisfies the corresponding inf-sup condition on $X \times M$. Finally, the unique solvability of (6) is a consequence of Theorem 2.34 in [28]. We omit further details. □

Remark 3 *At first glance, the corresponding discrete mixed formulation to* (6) *needs to satisfy a discrete version of the inf-sup condition. This implies that it is not possible to use any pair of the subspaces, in practice. In order to enlarge the choice of pairs of subspaces to approximate the exact solution, we propose a stabilized scheme in next section. In particular, we will follow an approach that allows us to relax the use of the rotation as an extra unknown.*

3 The augmented mixed finite element method

In this section, we analyse a stabilized formulation of problem (4)-(5). The fact that the displacement belongs actually to $[H^1(\Omega)]^2$, can be used in order to eliminate the rotation in (3). Indeed, proceeding as in [20], we define the *skew symmetric tensor* $\boldsymbol{\gamma}(\boldsymbol{v}) \,:=\, \frac{\nabla \boldsymbol{v} - (\nabla \boldsymbol{v})^{\mathtt{t}}}{2}$, for any $\boldsymbol{v} \in [H^1(\Omega)]^2$. This allows us to rewrite (3) as follows:

$$\frac{1}{2\,\mu}\boldsymbol{\sigma}^{\mathtt{d}} \,=\, \nabla \boldsymbol{u} \,-\, \boldsymbol{\gamma}(\boldsymbol{u}) \quad \text{in}\; \Omega\,. \tag{8}$$

In addition, there holds

$$\int_\Omega \gamma(\boldsymbol{v}) \,:\, \boldsymbol{\sigma} \,=\, 0 \quad \text{in } \Omega \quad \forall\, \boldsymbol{v} \in [H^1(\Omega)]^2\,, \tag{9}$$

thanks to the symmetry of $\boldsymbol{\sigma}$. These equations allow us to introduce the following mixed variational formulation for the first order system (1): *Find* $(\boldsymbol{\sigma}, \boldsymbol{u}) \in H_0(\mathbf{div};\Omega) \times [H^1(\Omega)]^2$ *such that*

$$\frac{1}{2\,\mu}\int_\Omega \boldsymbol{\sigma}^{\mathrm{d}} \,:\, \boldsymbol{\tau}^{\mathrm{d}} + \int_\Omega \boldsymbol{u}\cdot\mathbf{div}(\boldsymbol{\tau}) + \int_\Omega \gamma(\boldsymbol{u}) : \boldsymbol{\tau} \,=\, \langle \boldsymbol{\tau\nu}, \boldsymbol{g}\rangle_\Gamma \qquad \forall\,\boldsymbol{\tau} \in H_0(\mathbf{div};\Omega)\,, \tag{10}$$

$$-\int_\Omega \boldsymbol{v}\cdot\mathbf{div}(\boldsymbol{\sigma}) - \int_\Omega \gamma(\boldsymbol{v}) \,:\, \boldsymbol{\sigma} \,=\, \int_\Omega \boldsymbol{f}\cdot\boldsymbol{v} \qquad \forall\,\boldsymbol{v} \in [H^1(\Omega)]^2. \tag{11}$$

Now, we proceed as in [31], and include the least-squares terms given by

$$\kappa_1 \int_\Omega \Big(\boldsymbol{\varepsilon}(\boldsymbol{u}) - \frac{1}{2\,\mu}\boldsymbol{\sigma}^{\mathrm{d}}\Big) \,:\, \Big(\boldsymbol{\varepsilon}(\boldsymbol{v}) + \frac{1}{2\,\mu}\boldsymbol{\tau}^{\mathrm{d}}\Big) = 0 \qquad \forall\,(\boldsymbol{\tau},\boldsymbol{v}) \in H(\mathbf{div};\Omega)\times[H^1(\Omega)]^2\,, \tag{12}$$

$$\kappa_2 \int_\Omega \mathbf{div}(\boldsymbol{\sigma})\cdot\mathbf{div}(\boldsymbol{\tau}) \,=\, -\,\kappa_2\int_\Omega \boldsymbol{f}\cdot\mathbf{div}(\boldsymbol{\tau}) \qquad \forall \boldsymbol{\tau} \in H(\mathbf{div};\Omega)\,, \tag{13}$$

$$\kappa_3 \int_\Gamma \boldsymbol{u}\cdot\boldsymbol{v} = \kappa_3 \int_\Gamma \boldsymbol{g}\cdot\boldsymbol{v} \quad \forall\,\boldsymbol{v} \in [H^1(\Omega)]^2\,, \tag{14}$$

with $\kappa_1, \kappa_2, \kappa_3 \in \mathbb{R}$ at our disposal.

In what follows, we denote by $\boldsymbol{H} \,:=\, H(\mathbf{div};\Omega)\times[H^1(\Omega)]^2$ and $\boldsymbol{H}_0 := H_0(\mathbf{div};\Omega)\times[H^1(\Omega)]^2 \,\subseteq\, \boldsymbol{H}$. We provide $\boldsymbol{H}$ with the inner product

$$\langle(\boldsymbol{\rho},\boldsymbol{z}),(\boldsymbol{\tau},\boldsymbol{v})\rangle_{\boldsymbol{H}} \,:=\, (\boldsymbol{\rho},\boldsymbol{\tau})_{H(\mathbf{div};\Omega)} + (\boldsymbol{z},\boldsymbol{v})_{[H^1(\Omega)]^2} \quad \forall\,(\boldsymbol{\rho},\boldsymbol{z}),(\boldsymbol{\tau},\boldsymbol{v}) \in \boldsymbol{H}\times\boldsymbol{H}\,,$$

which induces the norm $||\cdot||_{\boldsymbol{H}} \,:\, \boldsymbol{H} \to \mathbb{R}$, given by

$$\|(\boldsymbol{\tau},\boldsymbol{v})\|_{\boldsymbol{H}} \,:=\, \Big(\|\boldsymbol{\tau}\|^2_{H(\mathbf{div};\Omega)} + \|\boldsymbol{v}\|^2_{[H^1(\Omega)]^2}\Big)^{1/2} \quad \forall\,(\boldsymbol{\tau},\boldsymbol{v}) \,\in\, \boldsymbol{H}\,.$$

Then, adding the equations (10), (11), (12), (13) and (14), we obtain the following augmented mixed scheme: *Find* $(\boldsymbol{\sigma},\boldsymbol{u}) \in \boldsymbol{H}_0$ *such that*

$$A((\boldsymbol{\sigma},\boldsymbol{u}),(\boldsymbol{\tau},\boldsymbol{v})) \,=\, F(\boldsymbol{\tau},\boldsymbol{v})\,, \quad \forall\,(\boldsymbol{\tau},\boldsymbol{v}) \,\in\, \boldsymbol{H}_0\,, \tag{15}$$

where the bilinear form $A \,:\, \boldsymbol{H}\times\boldsymbol{H} \to \mathbb{R}$ is given by

$$\begin{aligned} A((\boldsymbol{\rho},\boldsymbol{z}),(\boldsymbol{\tau},\boldsymbol{v})) \,:=\, & \frac{1}{2\,\mu}\int_\Omega \boldsymbol{\rho}^{\mathrm{d}} \,:\, \boldsymbol{\tau}^{\mathrm{d}} + \int_\Omega \boldsymbol{z}\cdot\mathbf{div}(\boldsymbol{\tau}) + \int_\Omega \boldsymbol{\tau} \,:\, \gamma(\boldsymbol{z}) \\ & - \int_\Omega \boldsymbol{v}\cdot\mathbf{div}(\boldsymbol{\rho}) - \int_\Omega \boldsymbol{\rho} \,:\, \gamma(\boldsymbol{v}) + \kappa_1 \int_\Omega \Big(\boldsymbol{\varepsilon}(\boldsymbol{z}) - \frac{1}{2\,\mu}\boldsymbol{\rho}^{\mathrm{d}}\Big) \,:\, \Big(\boldsymbol{\varepsilon}(\boldsymbol{v}) + \frac{1}{2\,\mu}\boldsymbol{\tau}^{\mathrm{d}}\Big) \\ & + \kappa_2 \int_\Omega \mathbf{div}(\boldsymbol{\rho})\cdot\mathbf{div}(\boldsymbol{\tau}) + \kappa_3 \int_\Gamma \boldsymbol{z}\cdot\boldsymbol{v} \quad \forall\,(\boldsymbol{\rho},\boldsymbol{z}),(\boldsymbol{\tau},\boldsymbol{v}) \in \boldsymbol{H}\times\boldsymbol{H}\,, \end{aligned}$$

and the linear functional $F : \boldsymbol{H} \to \mathbb{R}$ is defined by

$$F(\boldsymbol{\tau}, \boldsymbol{v}) \,:=\, \int_\Omega \boldsymbol{f} \cdot (\, \boldsymbol{v} \,-\, \kappa_2 \,\mathbf{div}(\boldsymbol{\tau})\,) \,+\, \kappa_3 \int_\Gamma \boldsymbol{g} \cdot \boldsymbol{v} \,+\, \langle \boldsymbol{\tau\nu}, \boldsymbol{g} \rangle_\Gamma \quad \forall\, (\boldsymbol{\tau}, \boldsymbol{v}) \in \boldsymbol{H}\,.$$

At this point, we recall the following important result, which is another type of Korn's inequality.

Lemma 4 *There exists $c_2 > 0$, depending only on Ω, such that*

$$\forall\, \boldsymbol{z} \,\in\, [H^1(\Omega)]^2 \,:\, c_2\, ||\boldsymbol{z}||_{[H^1(\Omega)]^2} \,\leq\, ||\boldsymbol{\varepsilon}(\boldsymbol{z})||_{[L^2(\Omega)]^{2\times 2}} \,+\, ||\boldsymbol{z}||_{[L^2(\Gamma)]^2}\,. \tag{16}$$

Proof. We refer to Lemma 3.1 in [32]. (16) is then derived as an application of this Lemma, considering the continuous mapping $p : [H^1(\Omega)]^2 \to \mathbb{R}$, given by $p(\boldsymbol{z}) \,:=\, ||\boldsymbol{z}||_{[L^2(\Gamma)]^2}$. □

Lemmas 1 and 4 will be helpful to characterize the values that can take the parameters $\kappa_1, \kappa_2, \kappa_3$ in order to ensure the boundedness of A in $\boldsymbol{H}$, and its strong coercivity on $\boldsymbol{H}_0$. As a result, we deduce that when the stabilization parameters $(\kappa_1, \kappa_2, \kappa_3)$ satisfy the following assumptions: $\kappa_1 \in (0, 2\,\mu)$, $\kappa_2 > 0$ and $\kappa_3 > 0$, then there exist positive constants M and α, such that

$$\begin{aligned} |A((\boldsymbol{\rho}, \boldsymbol{z}), (\boldsymbol{\tau}, \boldsymbol{v}))| \;&\leq M\, \|(\boldsymbol{\rho}, \boldsymbol{z})\|_{\boldsymbol{H}}\; \|(\boldsymbol{\tau}, \boldsymbol{v})\|_{\boldsymbol{H}}\,, \qquad \forall\, (\boldsymbol{\rho}, \boldsymbol{z}),\, (\boldsymbol{\tau}, \boldsymbol{v}) \in \boldsymbol{H}\,, \\ A((\boldsymbol{\tau}, \boldsymbol{v}), (\boldsymbol{\tau}, \boldsymbol{v})) \;&\geq \alpha\; \|(\boldsymbol{\tau}, \boldsymbol{v})\|^2_{\boldsymbol{H}}\,, \qquad \forall\, (\boldsymbol{\tau}, \boldsymbol{v}) \,\in\, \boldsymbol{H}_0\,. \end{aligned}$$

By invoking Lax-Milgram theorem, we can prove that the augmented variational formulation (15) has a unique solution $(\boldsymbol{\sigma}, \boldsymbol{u}) \,\in\, \boldsymbol{H}_0$. Moreover, there exists a positive constant C, such that

$$\|(\boldsymbol{\sigma}, \boldsymbol{u})\|_{\boldsymbol{H}} \,\leq\, C\, \left(\|\boldsymbol{f}\|_{[L^2(\Omega)]^2} + \|\boldsymbol{g}\|_{[H^{1/2}(\Gamma)]^2} \right)\,.$$

Now, let h be a positive parameter and consider the finite dimensional subspace $\boldsymbol{H}_{0,h} \subset \boldsymbol{H}_0$. Then, the discrete Galerkin scheme associated to problem (15) reads: *Find* $(\boldsymbol{\sigma}_h, \boldsymbol{u}_h) \,\in\, \boldsymbol{H}_{0,h}$ *such that*

$$A((\boldsymbol{\sigma}_h, \boldsymbol{u}_h), (\boldsymbol{\tau}_h, \boldsymbol{v}_h)) = F(\boldsymbol{\tau}_h, \boldsymbol{v}_h) \quad \forall\, (\boldsymbol{\tau}_h, \boldsymbol{v}_h) \in\, \boldsymbol{H}_{0,h}\,. \tag{17}$$

We remark that (17) is also uniquely solvable, for any $h > 0$, since we are dealing with conforming schemes. Next, we describe the analysis for a natural choice of $\boldsymbol{H}_{0,h}$ that preserves stability. In what follows, we assume that Ω is a polygonal region and let $\{\mathcal{T}_h\}_{h>0}$ be a regular family of triangulations of $\overline{\Omega}$ such that $\overline{\Omega} \,=\, \cup\{\, T \,:\, T \,\in\, \mathcal{T}_h\,\}$. Given a triangle $T \in \mathcal{T}_h$, we denote by h_T its diameter and define the mesh size $h := \max\{\, h_T \,:\, T \in \mathcal{T}_h\,\}$. In addition, given an integer $\ell \geq 0$ and a subset S of $\mathbb{R}^2$, we denote by $\mathcal{P}_\ell(S)$ the space of polynomials in two variables defined in S of total degree at most ℓ, and for each $T \in \mathcal{T}_h$, we define the local Raviart-Thomas space of order ℓ, as $\mathcal{RT}_\ell(T) \,:=\, [\mathcal{P}_\ell(T)]^2 \,\oplus\, \mathcal{P}_\ell(T)\,\boldsymbol{x} \,\subseteq\, [\mathcal{P}_{\ell+1}(T)]^2$, for all $\boldsymbol{x} \,\in\, T$. Next, we define the finite element subspaces

$$\begin{aligned} H^{\boldsymbol{\sigma}}_h \;&:=\; \left\{\, \boldsymbol{\tau}_h \in H(\mathbf{div}; \Omega) \,:\, \boldsymbol{\tau}_h|_T \,\in\, [\mathcal{RT}_\ell(T)^{\mathrm{t}}]^2 \quad \forall\, T \,\in\, \mathcal{T}_h \,\right\}\,, \\ H^{\boldsymbol{\sigma}}_{0,h} \;&:=\; \left\{\, \boldsymbol{\tau}_h \in H^{\boldsymbol{\sigma}}_h \,:\, \int_\Omega \mathrm{tr}(\boldsymbol{\tau}_h) \,=\, 0 \,\right\}\,, \\ H^{\boldsymbol{u}}_h \;&:=\; \left\{\, \boldsymbol{v}_h \,\in\, [\mathcal{C}(\overline{\Omega})]^2 \,:\, \boldsymbol{v}_h|_T \,\in\, [\mathcal{P}_{\ell+1}(T)]^2 \quad \forall\, T \,\in\, \mathcal{T}_h \,\right\}\,. \end{aligned}$$

Then, a family of stable finite element subspaces is given by

$$\boldsymbol{H}_{0,h} \,:=\, H_{0,h}^{\boldsymbol{\sigma}} \times H_h^{\boldsymbol{u}} \,.$$

Under the assumption that $\{\mathcal{T}_h\}_{h>0}$ is shape-regular, the Galerkin scheme (17) is well-posed, and a Céa estimate can be obtained. In addition, the corresponding rate of convergence of the Galerkin scheme (17), for this particular choice of finite element subspaces, is presented in the next theorem.

Theorem 5 *Let $(\boldsymbol{\sigma}, \boldsymbol{u}) \in \boldsymbol{H}_0$ and $(\boldsymbol{\sigma}_h, \boldsymbol{u}_h) \in \boldsymbol{H}_{0,h}$ be the unique solutions of problems* (15) *and* (17)*, respectively. In addition, assume that $\boldsymbol{\sigma} \in [H^r(\Omega)]^{2\times 2}$, $\mathbf{div}(\boldsymbol{\sigma}) \in [H^r(\Omega)]^2$ and $\boldsymbol{u} \in [H^{r+1}(\Omega)]^2$, for some $r \in (0, \ell+1]$. Then, there exists $C > 0$, independent of h, such that there holds*

$$\|(\boldsymbol{\sigma}, \boldsymbol{u}) - (\boldsymbol{\sigma}_h, \boldsymbol{u}_h)\|_{\boldsymbol{H}} \,\leq\, C\, h^r \,\left(\|\boldsymbol{\sigma}\|_{[H^r(\Omega)]^{2\times 2}} \,+\, \|\mathbf{div}(\boldsymbol{\sigma})\|_{[H^r(\Omega)]^2} \,+\, \|\boldsymbol{u}\|_{[H^{r+1}(\Omega)]^2} \right) \,.$$

Proof. It is a consequence of Céa's estimate and the corresponding well known approximation properties. We omit further details. □

4 A posteriori error analysis

In this section, we partially follow the ideas developed in [7] and [10] (see also, [13], [14] and [8]), and we obtain a residual-based a posteriori error analysis of the augmented mixed finite element method (17). We first introduce some notations and results concerning to the Clément and Raviart-Thomas interpolation operators.

4.1 Some notations and known results

Given $T \in \mathcal{T}_h$, we let $E(T)$ be the list of its edges, and let $\mathcal{E}_h$ be the list of all edges (counted once) induced by the triangulation $\mathcal{T}_h$. Then, we set $\mathcal{E}_h \,:=\, \mathcal{E}_h^{\mathtt{I}} \cup \mathcal{E}_h^{\partial}$, where $\mathcal{E}_h^{\mathtt{I}} \,:=\, \{e \in \mathcal{E}_h \,:\, e \subseteq \Omega\}$, and $\mathcal{E}_h^{\partial} \,:=\, \{e \in \mathcal{E}_h \,:\, e \subseteq \Gamma\}$. Also, for each edge $e \in \mathcal{E}_h$, we fix a unit normal vector $\boldsymbol{\nu}_e \,:=\, (\nu_1, \nu_2)^{\mathtt{t}}$, and let $\boldsymbol{t}_e \,:=\, (-\nu_2, \nu_1)^{\mathtt{t}}$ be the corresponding fixed unit tangential vector along e. From now on, when no confusion arises, we simply write $\boldsymbol{\nu}$ and $\boldsymbol{t}$ instead of $\boldsymbol{\nu}_e$ and $\boldsymbol{t}_e$, respectively. Finally, given a vector valued field $\boldsymbol{v} := (v_1, v_2)^{\mathtt{t}}$, we define

$$\underline{\mathbf{curl}}(\boldsymbol{v}) \,:=\, \begin{pmatrix} \frac{\partial v_1}{\partial x_2} & -\frac{\partial v_1}{\partial x_1} \\ \frac{\partial v_2}{\partial x_2} & -\frac{\partial v_2}{\partial x_1} \end{pmatrix} \,.$$

We will use the Clément interpolation operator $I_h \,:\, H^1(\Omega) \to \mathcal{C}(\overline{\Omega}) \,\cap\, \mathcal{P}_1(\mathcal{T}_h)$ (cf. [25]). A vector version of I_h, say $\boldsymbol{I}_h \,:\, [H^1(\Omega)]^2 \to H_h^{\boldsymbol{u}}$, which is defined component-wise by I_h, is also required. The following lemma establishes the local approximation properties of I_h.

Lemma 6 *There exist constants $c_1, c_2 > 0$, independent of h, such that for all $v \in H^1(\Omega)$ there holds*

$$||v - I_h(v)||_{H^m(T)} \,\leq\, c_1\, h_T^{1-m}\, |v|_{H^1(\omega(T))} \,, \quad \forall\, m \in \{0,1\}\,, \forall\, T \in \mathcal{T}_h \,,$$
$$||v - I_h(v)||_{L^2(e)} \,\leq\, c_2\, h_e^{1/2}\, |v|_{H^1(\omega(e))} \quad \forall\, e \in \mathcal{E}_h \,,$$

where $\omega(T) := \bigcup\{T' \in \mathcal{T}_h : \partial T' \cap \partial T \neq \emptyset\}$*,* h_e *denotes the length of the side* $e \in \mathcal{E}_h$*, and* $\omega(e) := \bigcup\{T' \in \mathcal{T}_h : \partial T' \cap e \neq \emptyset\}$ *.*

Proof. See [25]. □

We also need to introduce the Raviart-Thomas interpolation operator $\Pi_h^k : [H^1(\Omega)]^{2\times 2} \to \boldsymbol{H}_h^{\boldsymbol{\sigma}}$ as follows (cf. [19, 34]). Given $\boldsymbol{\tau} \in [H^1(\Omega)]^{2\times 2}$, $\Pi_h^k(\boldsymbol{\tau}) \in \boldsymbol{H}_h^{\boldsymbol{\sigma}}$ is uniquely characterized by the following conditions:

$$\int_e \Pi_h^k(\boldsymbol{\tau})\,\boldsymbol{\nu}\cdot\boldsymbol{q} \;=\; \int_e \boldsymbol{\tau}\,\boldsymbol{\nu}\cdot\boldsymbol{q}\,, \quad \forall e \in \mathcal{E}_h\,, \quad \forall \boldsymbol{q} \in [\mathcal{P}_k(e)]^2\,, \quad \text{when } k \geq 0\,, \tag{18}$$

$$\int_T \Pi_h^k(\boldsymbol{\tau}) : \boldsymbol{\rho} \;=\; \int_T \boldsymbol{\tau} : \boldsymbol{\rho}\,, \quad \forall T \in \mathcal{T}_h\,, \quad \forall \boldsymbol{\rho} \in [\mathcal{P}_{k-1}(T)]^{2\times 2}\,, \quad \text{when } k \geq 1\,. \tag{19}$$

The operator Π_h^k satisfies the following approximation properties.

Lemma 7 *There exist constants* $c_3, c_4, c_5 > 0$*, independent of* h*, such that for all* $T \in \mathcal{T}_h$*:*

$$||\boldsymbol{\tau} - \Pi_h^k(\boldsymbol{\tau})||_{[L^2(T)]^{2\times 2}} \;\leq\; c_3\, h_T^m\, |\boldsymbol{\tau}|_{[H^m(T)]^{2\times 2}} \quad \forall \boldsymbol{\tau} \in [H^m(\Omega)]^{2\times 2} \quad 1 \leq m \leq k+1 \tag{20}$$

and for all $\boldsymbol{\tau} \in [H^m(\Omega)]^{2\times 2}$ *with* $\mathbf{div}(\boldsymbol{\tau}) \in [H^m(\Omega)]^2$*,*

$$||\mathbf{div}(\boldsymbol{\tau} - \Pi_h^k(\boldsymbol{\tau}))||_{[L^2(T)]^2} \;\leq\; c_4\, h_T^m\, |\mathbf{div}(\boldsymbol{\tau})|_{[H^m(T)]^2} \quad 0 \leq m \leq k+1 \tag{21}$$

and

$$||\boldsymbol{\tau}\,\boldsymbol{\nu} - \Pi_h^k(\boldsymbol{\tau})\,\boldsymbol{\nu}||_{[L^2(e)]^2} \;\leq\; c_5\, h_e^{1/2}\, ||\boldsymbol{\tau}||_{[H^1(T_e)]^{2\times 2}} \quad \forall\, e \in \mathcal{E}_h\,, \quad \forall\, \boldsymbol{\tau} \in [H^1(\Omega)]^{2\times 2} \tag{22}$$

where $T_e \in \mathcal{T}_h$ *contains* e *on its boundary.*

Proof. We refer to [19] or [34]. □

Remark 8 *The interpolation operator* Π_h^k *can also be defined as a bounded linear operator from the larger space* $[H^s(\Omega)]^{2\times 2} \cap H(\mathbf{div};\Omega)$ *into* $H_h^{\boldsymbol{\sigma}}$*, for all* $s \in (0,1]$ *(see, e.g., Theorem 3.16 in [33]).*

Now we are ready to deduce a reliable a posteriori error estimator. First, we let $(\boldsymbol{\sigma}, \boldsymbol{u})$ and $(\boldsymbol{\sigma}_h, \boldsymbol{u}_h)$ be the unique solutions of problems (15) and (17), respectively. It is not difficult to establish the orthogonality relation

$$A((\boldsymbol{\sigma} - \boldsymbol{\sigma}_h, \boldsymbol{u} - \boldsymbol{u}_h), (\boldsymbol{\tau}_h, \boldsymbol{v}_h)) \;=\; 0 \quad \forall\, (\boldsymbol{\tau}_h, \boldsymbol{v}_h) \in \boldsymbol{H}_{0,h}\,. \tag{23}$$

We notice that for any $\delta \in \mathbb{R}$, there holds

$$\forall\, (\boldsymbol{\rho}, \boldsymbol{w}) \;\in\; \boldsymbol{H} \;:\; A((\boldsymbol{\rho}, \boldsymbol{w}), (\delta\,\boldsymbol{I}, \boldsymbol{0})) \;=\; 0 \quad \text{and} \quad F(\delta\,\boldsymbol{I}, \boldsymbol{0}) \;=\; 0\,.$$

This allows us to establish

$$A((\boldsymbol{\sigma}, \boldsymbol{u}), (\boldsymbol{\tau}, \boldsymbol{v})) \;=\; F(\boldsymbol{\tau}, \boldsymbol{v}) \quad \forall\, (\boldsymbol{\tau}, \boldsymbol{v}) \;\in\; \boldsymbol{H}\,. \tag{24}$$

Moreover, knowing that each $\boldsymbol{\zeta}_h \in H_h^{\boldsymbol{\sigma}}$ can be decomposed as $\boldsymbol{\zeta}_h = \boldsymbol{\zeta}_{0,h} + \lambda \boldsymbol{I}$, with $\boldsymbol{\zeta}_{0,h} \in H_{0,h}^{\boldsymbol{\sigma}}$ and $\lambda \in \mathbb{R}$, we deduce that

$$A((\boldsymbol{\sigma}_h, \boldsymbol{u}_h), (\boldsymbol{\zeta}_h, \boldsymbol{z}_h)) = F(\boldsymbol{\zeta}_h, \boldsymbol{z}_h) \quad \forall (\boldsymbol{\zeta}_h, \boldsymbol{z}_h) \in \boldsymbol{H}_h := H_h^{\boldsymbol{\sigma}} \times H_h^{\boldsymbol{u}} . \tag{25}$$

As a consequence, the standard orthogonality relation in $\boldsymbol{H}_{0,h}$ (23) can be extended onto $\boldsymbol{H}_h$, i.e.

$$A((\boldsymbol{\sigma} - \boldsymbol{\sigma}_h, \boldsymbol{u} - \boldsymbol{u}_h), (\boldsymbol{\zeta}_h, \boldsymbol{z}_h)) = 0 \quad \forall (\boldsymbol{\zeta}_h, \boldsymbol{z}_h) \in \boldsymbol{H}_h . \tag{26}$$

Next, we define the Ritz projection of the error with respect to the provided inner product of $\boldsymbol{H}$, as the unique element $(\bar{\boldsymbol{\sigma}}, \bar{\boldsymbol{u}}) \in \boldsymbol{H}$ such that

$$\langle (\bar{\boldsymbol{\sigma}}, \bar{\boldsymbol{u}}), (\boldsymbol{\tau}, \boldsymbol{v}) \rangle_{\boldsymbol{H}} = A((\boldsymbol{\sigma} - \boldsymbol{\sigma}_h, \boldsymbol{u} - \boldsymbol{u}_h), (\boldsymbol{\tau}, \boldsymbol{v})) \quad \forall (\boldsymbol{\tau}, \boldsymbol{v}) \in \boldsymbol{H} . \tag{27}$$

We remark that the existence and uniqueness of $(\bar{\boldsymbol{\sigma}}, \bar{\boldsymbol{u}}) \in \boldsymbol{H}$ is guaranteed by the Lax-Milgram theorem. On the other hand, invoking the strong coercivity of A on $\boldsymbol{H}_0$, we derive:

$$\begin{aligned} \alpha \, ||(\boldsymbol{\sigma} - \boldsymbol{\sigma}_h, \boldsymbol{u} - \boldsymbol{u}_h)||_{\boldsymbol{H}} &\leq \sup_{(\boldsymbol{\tau},\boldsymbol{v}) \in \boldsymbol{H}_0 \backslash \{(\mathbf{0},\mathbf{0})\}} \frac{A((\boldsymbol{\sigma} - \boldsymbol{\sigma}_h, \boldsymbol{u} - \boldsymbol{u}_h), (\boldsymbol{\tau}, \boldsymbol{v}))}{||(\boldsymbol{\tau}, \boldsymbol{v})||_{\boldsymbol{H}}} \\ &\leq \sup_{(\boldsymbol{\tau},\boldsymbol{v}) \in \boldsymbol{H} \backslash \{(\mathbf{0},\mathbf{0})\}} \frac{A((\boldsymbol{\sigma} - \boldsymbol{\sigma}_h, \boldsymbol{u} - \boldsymbol{u}_h), (\boldsymbol{\tau}, \boldsymbol{v}))}{||(\boldsymbol{\tau}, \boldsymbol{v})||_{\boldsymbol{H}}} = ||(\bar{\boldsymbol{\sigma}}, \bar{\boldsymbol{u}})||_{\boldsymbol{H}} . \end{aligned} \tag{28}$$

Then, in order to obtain a reliable a posteriori error estimator for the discrete scheme (17), it is enough to bound from above $||(\bar{\boldsymbol{\sigma}}, \bar{\boldsymbol{u}})||_{\boldsymbol{H}}$, i.e. the last supremum in (28). Thanks to (26) and (24), we derive

$$\begin{aligned} \forall ((\boldsymbol{\tau}, \boldsymbol{v}), (\boldsymbol{\zeta}_h, \boldsymbol{z}_h)) \in \boldsymbol{H} \times \boldsymbol{H}_h : \; & A((\boldsymbol{\sigma} - \boldsymbol{\sigma}_h, \boldsymbol{u} - \boldsymbol{u}_h), (\boldsymbol{\tau}, \boldsymbol{v})) \\ &= F((\boldsymbol{\tau} - \boldsymbol{\zeta}_h, \boldsymbol{v} - \boldsymbol{z}_h)) - A((\boldsymbol{\sigma}_h, \boldsymbol{u}_h), (\boldsymbol{\tau} - \boldsymbol{\zeta}_h, \boldsymbol{v} - \boldsymbol{z}_h)) . \end{aligned} \tag{29}$$

Our next aim relies on choosing the appropriate $(\boldsymbol{\zeta}_h, \boldsymbol{z}_h) \in \boldsymbol{H}_h$, that leads us to our estimator. To achieve this, we recall the following result, which establishes a quasi-Helmholtz decomposition of functions in $H(\mathbf{div}; \Omega)$.

Lemma 9 *For each $\boldsymbol{\tau} \in H(\mathbf{div}; \Omega)$, there exist $\boldsymbol{\chi} \in [H^1(\Omega)]^2$ and $\boldsymbol{\Phi} \in [H_0^1(\Omega)]^{2\times 2}$, such that*

$$\boldsymbol{\tau} = \underline{\mathbf{curl}}(\boldsymbol{\chi}) + \boldsymbol{\Phi} + \frac{1}{2} \boldsymbol{d} \otimes (x_1 - a, x_2 - b)^{\mathtt{t}} , \tag{30}$$

where $(a, b)^{\mathtt{t}}$ is any fixed point belonging to Ω, and $\boldsymbol{d} := (d_1, d_2)^{\mathtt{t}}$ with $d_i := \frac{1}{|\Omega|} \int_\Omega \operatorname{div}((\tau_{i1}, \tau_{i2})^{\mathtt{t}})$, $i \in \{1, 2\}$. In addition, there exists $C > 0$, such that

$$|\boldsymbol{\chi}|^2_{[H^1(\Omega)]^2} + \|\boldsymbol{\Phi}\|^2_{[H^1(\Omega)]^{2\times 2}} \leq C \, \|\boldsymbol{\tau}\|^2_{H(\mathbf{div};\Omega)} . \tag{31}$$

Proof. We refer to [5] (cf. Lemma 7). $\square$

Now, we take $(\boldsymbol{\tau}, \boldsymbol{v}) \in \boldsymbol{H}$. Since $\boldsymbol{\tau} \in H(\mathbf{div};\Omega)$, we consider $\boldsymbol{\chi} \in [H^1(\Omega)]^2$ and $\boldsymbol{\Phi} \in [H_0^1(\Omega)]^{2\times 2}$ as provided in Lemma 9. Next, we need a suitable choice of $\boldsymbol{\tau}_h \in H_h^{\boldsymbol{\sigma}}$. To this aim, we set $\boldsymbol{\chi}_h := \boldsymbol{I}_h(\boldsymbol{\chi})$, and define

$$\boldsymbol{\tau}_h \,:=\, \underline{\mathbf{curl}}(\boldsymbol{\chi}_h) \,+\, \Pi_h^\ell(\boldsymbol{\Phi}) \,+\, \frac{1}{2}\,\boldsymbol{d} \otimes (x_1 - a, x_2 - b)^{\mathtt{t}} \,\in\, H_h^{\boldsymbol{\sigma}} \,. \tag{32}$$

We refer to (32) as a *discrete quasi-Helmholtz decomposition* of $\boldsymbol{\tau}$. Therefore, we can write

$$\boldsymbol{\tau} - \boldsymbol{\tau}_h \,=\, \underline{\mathbf{curl}}(\boldsymbol{\chi} - \boldsymbol{\chi}_h) \,+\, \boldsymbol{\Phi} - \Pi_h^\ell(\boldsymbol{\Phi})\,, \tag{33}$$

Now, invoking (29), with $\boldsymbol{\zeta}_h := \boldsymbol{\tau}_h$ and $\boldsymbol{z}_h := \boldsymbol{I}_h(\boldsymbol{v})$, we deduce that

$$A((\boldsymbol{\sigma} - \boldsymbol{\sigma}_h, \boldsymbol{u} - \boldsymbol{u}_h), (\boldsymbol{\tau}, \boldsymbol{v})) \,=\, F_1(\boldsymbol{\chi}) \,+\, F_2(\boldsymbol{\Phi}) \,+\, F_3(\boldsymbol{v})\,, \tag{34}$$

where $F_1, F_3 : [H^1(\Omega)]^2 \to \mathbb{R}$ and $F_2 : [H^1(\Omega)]^{2\times 2} \to \mathbb{R}$ are the linear functionals defined by

$$\begin{aligned}
F_1(\boldsymbol{\chi}) \,:=\, & -\int_\Omega \left(\frac{1}{2\,\mu}\boldsymbol{\sigma}_h^{\mathtt{d}} - \boldsymbol{\varepsilon}(\boldsymbol{u}_h)\right) : \underline{\mathbf{curl}}(\boldsymbol{\chi} - \boldsymbol{\chi}_h) \\
& - \frac{\kappa_1}{2\,\mu}\int_\Omega \left(\boldsymbol{\varepsilon}(\boldsymbol{u}_h) - \frac{1}{2\,\mu}\boldsymbol{\sigma}_h^{\mathtt{d}}\right) : \underline{\mathbf{curl}}(\boldsymbol{\chi} - \boldsymbol{\chi}_h)^{\mathtt{d}} \,+\, \langle \underline{\mathbf{curl}}(\boldsymbol{\chi} - \boldsymbol{\chi}_h)\,\boldsymbol{\nu}, \boldsymbol{g} - \boldsymbol{u}_h\rangle_\Gamma\,, \\
F_2(\boldsymbol{\Phi}) \,:=\, & -\kappa_2 \int_\Omega (\boldsymbol{f} + \mathbf{div}(\boldsymbol{\sigma}_h)) \cdot \mathbf{div}(\boldsymbol{\Phi} - \Pi_h^\ell(\boldsymbol{\Phi})) \,-\, \int_\Omega \left(\frac{1}{2\,\mu}\boldsymbol{\sigma}_h^{\mathtt{d}} - \boldsymbol{\varepsilon}(\boldsymbol{u}_h)\right) : (\boldsymbol{\Phi} - \Pi_h^\ell(\boldsymbol{\Phi})) \\
& - \frac{\kappa_1}{2\,\mu}\int_\Omega \left(\boldsymbol{\varepsilon}(\boldsymbol{u}_h) - \frac{1}{2\,\mu}\boldsymbol{\sigma}_h^{\mathtt{d}}\right) : (\boldsymbol{\Phi} - \Pi_h^\ell(\boldsymbol{\Phi}))^{\mathtt{d}}\,, \\
F_3(\boldsymbol{v}) \,:=\, & \int_\Omega (\boldsymbol{f} + \mathbf{div}(\boldsymbol{\sigma}_h)) \cdot (\boldsymbol{v} - \boldsymbol{I}_h(\boldsymbol{v})) \,-\, \kappa_1 \int_\Omega \left(\boldsymbol{\varepsilon}(\boldsymbol{u}_h) - \frac{1}{2\,\mu}\,\boldsymbol{\sigma}_h^{\mathtt{d}}\right) : \boldsymbol{\epsilon}(\boldsymbol{v} - \boldsymbol{I}_h(\boldsymbol{v})) \\
& + \frac{1}{2}\int_\Omega (\boldsymbol{\sigma}_h - \boldsymbol{\sigma}_h^{\mathtt{t}}) : \boldsymbol{\gamma}(\boldsymbol{v} - \boldsymbol{I}_h(\boldsymbol{v})) \,+\, \kappa_3 \int_\Gamma (\boldsymbol{g} - \boldsymbol{u}_h) \cdot (\boldsymbol{v} - \boldsymbol{I}_h(\boldsymbol{v}))\,.
\end{aligned}$$

Next, we proceed to bound each one of the three linear functionals.

Lemma 10 *Under the additional assumption that $\boldsymbol{g} \in [H^1(\Gamma)]^2$, there exists $C_1 > 0$, independent of h, such that*

$$|F_1(\boldsymbol{\chi})| \,\le\, C_1 \left(\sum_{T\in\mathcal{T}_h}\left\{\left\|\frac{1}{2\,\mu}\boldsymbol{\sigma}_h^{\mathtt{d}} - \boldsymbol{\varepsilon}(\boldsymbol{u}_h)\right\|_{[L^2(T)]^{2\times 2}}^2 + \sum_{e\in\mathcal{E}_h^\partial\cap\partial T} h_e \left\|\frac{d\boldsymbol{g}}{d\boldsymbol{t}} - \frac{d\boldsymbol{u}_h}{d\boldsymbol{t}}\right\|_{[L^2(e)]^2}^2\right\}\right)^{1/2} |\boldsymbol{\chi}|_{[H^1(\Omega)]^2}\,.$$

Proof. It relies on applying Cauchy-Schwarz inequality and notice that $\langle \underline{\mathbf{curl}}(\boldsymbol{\chi} - \boldsymbol{\chi}_h)\,\boldsymbol{\nu}, \boldsymbol{g} - \boldsymbol{u}_h\rangle_\Gamma = \langle \frac{d\boldsymbol{g}}{d\boldsymbol{t}} - \frac{d\boldsymbol{u}_h}{d\boldsymbol{t}}, \boldsymbol{\chi} - \boldsymbol{\chi}_h\rangle_\Gamma$. After that, we invoke Lemma 6 to conclude the proof. $\square$

Lemma 11 *There exists $C_2 > 0$, independent of h, such that*

$$|F_2(\boldsymbol{\Phi})| \,\le\, C_2 \left(\sum_{T\in\mathcal{T}_h} h_T^2 \left\|\frac{1}{2\,\mu}\boldsymbol{\sigma}_h^{\mathtt{d}} - \boldsymbol{\varepsilon}(\boldsymbol{u}_h)\right\|_{[L^2(T)]^{2\times 2}}^2 + \kappa_2^2\,||\boldsymbol{f} + \mathbf{div}(\boldsymbol{\sigma}_h)||_{[L^2(T)]^2}^2\right)^{1/2} |\boldsymbol{\Phi}|_{[H^1(\Omega)]^{2\times 2}}\,.$$

Proof. After invoking Cauchy-Schwarz inequality, we apply Lemma 7 to deduce the estimate. □

Taking into account Lemma 6 and the properties

$$\forall\, \boldsymbol{\tau} \in H(\mathbf{div};\Omega) \,:\, ||\boldsymbol{\tau}^{\mathtt{d}}||_{[L^2(\Omega)]^{2\times 2}} \,\leq\, ||\boldsymbol{\tau}||_{[L^2(\Omega)]^{2\times 2}}\,, \tag{35}$$

$$\forall\, \boldsymbol{v} \in [H^1(\Omega)]^2 \,:\, ||\boldsymbol{\varepsilon}(\boldsymbol{v})||^2_{[L^2(\Omega)]^{2\times 2}} + ||\boldsymbol{\gamma}(\boldsymbol{v})||^2_{[L^2(\Omega)]^{2\times 2}} \,=\, |\boldsymbol{v}|^2_{[H^1(\Omega)]^2}\,, \tag{36}$$

we can prove the boundedness of F_3, which is stated next.

Lemma 12 *There exists $C_3 > 0$, independent of h, such that*

$$|F_3(\boldsymbol{v})| \,\leq C_3 \left(\sum_{T\in\mathcal{T}_h} \left\{ h_T^2\, ||\boldsymbol{f} + \mathbf{div}(\boldsymbol{\sigma}_h)||^2_{[L^2(T)]^2} \,+\, \kappa_1^2 \left\| \frac{1}{2\,\mu}\boldsymbol{\sigma}_h^{\mathtt{d}} - \boldsymbol{\varepsilon}(\boldsymbol{u}_h) \right\|^2_{[L^2(T)]^{2\times 2}} \right\} \right.$$
$$\left. + \sum_{T\in\mathcal{T}_h} \left\{ ||\boldsymbol{\sigma}_h - \boldsymbol{\sigma}_h^{\mathtt{t}}||^2_{[L^2(T)]^{2\times 2}} \,+ \sum_{e\in\mathcal{E}_h^{\partial}\cap\partial T} \kappa_3^2\, h_e\, ||\boldsymbol{g} - \boldsymbol{u}_h||^2_{[L^2(e)]^2} \right\} \right)^{1/2} |\boldsymbol{v}|_{[H^1(\Omega)]^2}\,.$$

Lemmas 10, 11 and 12 help us to derive a residual a posteriori error estimator, which results to be reliable. This is the statement of the next theorem.

Theorem 13 *Assuming that $\boldsymbol{g} \in [H^1(\Gamma)]^2$, there exists $C_{\mathtt{rel}} > 0$, independent of h, such that*

$$||(\boldsymbol{\sigma} - \boldsymbol{\sigma}_h, \boldsymbol{u} - \boldsymbol{u}_h)||_{\boldsymbol{H}} \,\leq\, C_{\mathtt{rel}}\,\eta\,, \tag{37}$$

where $\eta := \left(\sum_{T\in\mathcal{T}_h} \eta_T^2 \right)^{1/2}$*, such that for any $T \in \mathcal{T}_h$*

$$\eta_T^2 \,:=\, \max\{\kappa_2^2, h_T^2\}\, ||\boldsymbol{f} + \mathbf{div}(\boldsymbol{\sigma}_h)||^2_{[L^2(T)]^2} \,+\, \max\{1, \kappa_1^2, h_T^2\} \left\| \boldsymbol{\varepsilon}(\boldsymbol{u}_h) - \frac{1}{2\,\mu}\,\boldsymbol{\sigma}_h^{\mathtt{d}} \right\|^2_{[L^2(T)]^{2\times 2}}$$
$$+\, \|\boldsymbol{\sigma}_h - \boldsymbol{\sigma}_h^{\mathtt{t}}\|^2_{[L^2(T)]^{2\times 2}} \,+ \sum_{e\in\mathcal{E}_h^{\partial}\cap\partial T} \left\{ h_e\, ||\boldsymbol{g} - \boldsymbol{u}_h||^2_{[L^2(e)]^2} \,+\, \kappa_3^2\, h_e \left\| \frac{d\boldsymbol{g}}{d\boldsymbol{t}} - \frac{d\boldsymbol{u}_h}{d\boldsymbol{t}} \right\|^2_{[L^2(e)]^2} \right\}. \tag{38}$$

A result on the local efficiency of our estimator, is given next.

Theorem 14 *Assuming that $\boldsymbol{g}$ is a continuous piecewise polynomial, there exists $C_{\mathtt{eff}} > 0$, independent of h, such that for any $T \in \mathcal{T}_h$ there holds*

$$C_{\mathtt{eff}}\,\eta_T \,\leq\, ||(\boldsymbol{\sigma} - \boldsymbol{\sigma}_h, \boldsymbol{u} - \boldsymbol{u}_h)||_{H(\mathbf{div};T)\times[H^1(T)]^2}\,. \tag{39}$$

Proof. The volumetric terms that define η_T (cf. (38)) are quite direct to bound from above. To deal with the last term in (38), we require to introduce the very well-known edge-bubble functions and a standard extension operator. The arguments are similar to the ones described in [8] and [7]. We omit further details. □

5 Mixed Boundary conditions

In this section, we continue assuming that the domain Ω has a polygonal boundary $\Gamma := \partial\Omega$, but now it may consist of two parts: $\Gamma_D \subseteq \Gamma$, close, with $|\Gamma_D| > 0$, and $\Gamma_N := \Gamma \setminus \Gamma_D$. Moreover, we will use the same notations related to Sobolev spaces, as introduced in Section 3.

Next, we consider the incompressibility elasticity problem: *Find the stress tensor $\hat{\boldsymbol{\sigma}}$, the displacement field $\boldsymbol{u}$ and the hydrostatic pressure p such that*

$$\begin{cases} \hat{\boldsymbol{\sigma}} & = 2\,\mu\,\boldsymbol{\varepsilon}(\boldsymbol{u}) + p\,\boldsymbol{I} \quad \text{in} \quad \Omega\,, \\ -\,\mathbf{div}(\hat{\boldsymbol{\sigma}}) & = \boldsymbol{f} \quad \text{in} \quad \Omega\,, \\ \operatorname{div}(\boldsymbol{u}) & = 0 \quad \text{in} \quad \Omega\,, \\ \boldsymbol{u} & = \mathbf{0} \quad \text{on} \quad \Gamma_D\,, \\ \hat{\boldsymbol{\sigma}}\,\boldsymbol{\nu} & = \boldsymbol{g} \quad \text{on} \quad \Gamma_N\,, \end{cases} \tag{40}$$

where the external body force $\boldsymbol{f}$ belongs to $[L^2(\Omega)]^{2\times 2}$, and the traction $\boldsymbol{g} \in [H_{00}^{-1/2}(\Gamma_N)]^2$, which is the dual space of $[H_{00}^{1/2}(\Gamma_N)]^2 := \left\{ \boldsymbol{v}|_{\Gamma_N} : \boldsymbol{v} \in [H^1_{\Gamma_D}(\Omega)]^2 \right\}$. Thanks to Korn's inequality on $[H^1_{\Gamma_D}(\Omega)]^2$ (cf. Chapter VI in [18]), there exists a unique $\boldsymbol{z} \in [H^1_{\Gamma_D}(\Omega)]^2$ such that

$$\mathbf{div}(\boldsymbol{\varepsilon}(\boldsymbol{z})) = \mathbf{0} \quad \text{in} \quad \Omega\,, \quad \boldsymbol{z} = \mathbf{0} \quad \text{on} \quad \Gamma_D\,, \quad \boldsymbol{\varepsilon}(\boldsymbol{z})\,\boldsymbol{\nu} = \boldsymbol{g} \quad \text{on} \quad \Gamma_N\,. \tag{41}$$

In addition, there exists $\tilde{C} > 0$, such that $||\boldsymbol{z}||_{[H^1(\Omega)]^2} \leq \tilde{C}\,||\boldsymbol{g}||_{[H_{00}^{-1/2}(\Gamma_N)]^2}$. This allows us to set $\widehat{\boldsymbol{\sigma}}_{\boldsymbol{g}} := \boldsymbol{\varepsilon}(\boldsymbol{z}) \in \tilde{H}_N := \{\boldsymbol{\tau} \in H(\mathbf{div};\Omega) : \boldsymbol{\tau}\,\boldsymbol{\nu} = \mathbf{0} \quad \text{on} \quad \Gamma_N\}$, with $\mathbf{div}(\widehat{\boldsymbol{\sigma}}_{\boldsymbol{g}}) = \mathbf{0}$ in Ω. Then, introducing $\hat{\boldsymbol{\sigma}} := \boldsymbol{\sigma} + \widehat{\boldsymbol{\sigma}}_{\boldsymbol{g}}$, (40) can be written as

$$\begin{cases} -\,\mathbf{div}(\boldsymbol{\sigma}) & = \boldsymbol{f} \quad \text{in} \quad \Omega\,, \\ \frac{1}{2\,\mu}\,\boldsymbol{\sigma}^{\mathtt{d}} & = \boldsymbol{\nabla}\boldsymbol{u} - \gamma(\boldsymbol{u}) + \boldsymbol{\zeta} \quad \text{in} \quad \Omega\,, \\ \operatorname{div}(\boldsymbol{u}) & = 0 \quad \text{in} \quad \Omega\,, \\ \boldsymbol{u} & = \mathbf{0} \quad \text{on} \quad \Gamma_D\,, \\ \boldsymbol{\sigma}\,\boldsymbol{\nu} & = \mathbf{0} \quad \text{on} \quad \Gamma_N\,, \end{cases} \tag{42}$$

where $\boldsymbol{\zeta} := -\frac{1}{2\,\mu}\widehat{\boldsymbol{\sigma}}^{\mathtt{d}}_{\boldsymbol{g}}$. We notice that the hydrostatic pressure is recovered from $p = \frac{1}{2}\operatorname{tr}(\hat{\boldsymbol{\sigma}})$. Next, proceeding in standard way, we deduce the following variational formulation of (42): *Find* $(\boldsymbol{\sigma}, \boldsymbol{u}, \gamma) \in \tilde{H}_N \times [L^2(\Omega)]^2 \times [L^2(\Omega)]^{2\times 2}_{\mathtt{skew}}$ *such that*

$$a(\boldsymbol{\sigma},\boldsymbol{\tau}) + b(\boldsymbol{\tau},(\boldsymbol{u},\gamma)) = F(\boldsymbol{\tau}) \quad \forall\,\boldsymbol{\tau} \in \tilde{H}_N\,, \tag{43}$$

$$b(\boldsymbol{\sigma},(\boldsymbol{v},\boldsymbol{\eta})) = G(\boldsymbol{v},\boldsymbol{\eta}) \quad \forall\,(\boldsymbol{v},\boldsymbol{\eta}) \in [L^2(\Omega)]^2 \times [L^2(\Omega)]^{2\times 2}_{\mathtt{skew}}\,, \tag{44}$$

where bilinear forms $a : \tilde{H}_N \times \tilde{H}_N \to \mathbb{R}$ and $b : \tilde{H}_N \times ([L^2(\Omega)]^2 \times [L^2(\Omega)]^{2\times 2}_{\mathtt{skew}}) \to \mathbb{R}$ are given by

$$\begin{aligned} a(\boldsymbol{\rho}, \boldsymbol{\tau}) &:= \frac{1}{2\,\mu} \int_\Omega \boldsymbol{\rho}^{\mathtt{d}} : \boldsymbol{\tau}^{\mathtt{d}} \quad \forall\, \boldsymbol{\rho}, \boldsymbol{\tau} \in \tilde{H}_N \,, \\ b(\boldsymbol{\rho}, (\boldsymbol{v}, \boldsymbol{\eta})) &:= -\int_\Omega \boldsymbol{v} \cdot \mathbf{div}(\boldsymbol{\rho}) - \int_\Omega \boldsymbol{\eta} : \boldsymbol{\rho} \quad \forall\, \boldsymbol{\rho} \in \tilde{H}_N \,, \forall\, (\boldsymbol{v}, \boldsymbol{\eta}) \in [L^2(\Omega)]^2 \times [L^2(\Omega)]^{2\times 2}_{\mathtt{skew}} \,, \end{aligned}$$

while the linear functionals $F : \tilde{H}_N \to \mathbb{R}$ and $G : [L^2(\Omega)]^2 \times [L^2(\Omega)]^{2\times 2}_{\mathtt{skew}} \to \mathbb{R}$ are defined as

$$\begin{aligned} F(\boldsymbol{\tau}) &:= \int_\Omega \boldsymbol{\zeta} : \boldsymbol{\tau} \quad \forall\, \boldsymbol{\tau} \in \tilde{H}_N \,, \\ G(\boldsymbol{v}, \boldsymbol{\eta}) &:= \int_\Omega \boldsymbol{f} \cdot \boldsymbol{v} \quad \forall\, (\boldsymbol{v}, \boldsymbol{\eta}) \in [L^2(\Omega)]^2 \times [L^2(\Omega)]^{2\times 2}_{\mathtt{skew}} \,. \end{aligned}$$

We recall the following result, that will be helpful for establishing the unique solvability of (43)-(44). Before that, we remark that given $\boldsymbol{\tau} \in \tilde{H}_N$, we can decomposed it as $\boldsymbol{\tau} := \boldsymbol{\tau}_0 + \lambda\,\boldsymbol{I}$, with $\boldsymbol{\tau}_0 \in H_0(\mathbf{div};\Omega)$ and $\lambda \in \mathbb{R}$ such that $\boldsymbol{\tau}\,\boldsymbol{\nu} = \mathbf{0}$ on Γ_N.

Lemma 15 *There exists $c_3 > 0$, depending only on Ω and Γ_N, such that*

$$\forall\, \boldsymbol{\tau} \in \tilde{H}_N : c_3\, ||\boldsymbol{\tau}||_{H(\mathbf{div};\Omega)} \le ||\boldsymbol{\tau}_0||_{H(\mathbf{div};\Omega)} \,. \tag{45}$$

Proof. We refer to Lemma 2.2 in [31]. □

Theorem 16 *Problem* (43)-(44) *has a unique solution, which satisfies the continuous dependency of the data property.*

Proof. First, we notice that the boundedness of a, b, F, and G, are straighforward. In addition, we have

$$\begin{aligned} W := \mathrm{Ker}(b) &:= \{\boldsymbol{\tau} \in \tilde{H}_N : b(\boldsymbol{\tau}, (\boldsymbol{v}, \boldsymbol{\eta})) = 0 \quad \forall\, (\boldsymbol{v}, \boldsymbol{\eta}) \in [L^2(\Omega)]^2 \times [L^2(\Omega)]^{2\times 2}_{\mathtt{skew}}\} \\ &= \{\boldsymbol{\tau} \in \tilde{H}_N : \boldsymbol{\tau} = \boldsymbol{\tau}^{\mathtt{t}} \quad \text{and} \quad \mathbf{div}(\boldsymbol{\tau}) = \mathbf{0} \quad \text{on} \quad \Omega\} \,. \end{aligned}$$

Then, with the help of Lemma 15, we can deduce the W-ellipticity of a. We point out that the inf-sup condition of b has been proved in Lemma 4.3 in [3]. Thus, invoking the very well-known Babuška-Brezzi theory, we conclude the unique solvability of (43)-(44). In addition, invoking the continuous dependence property, we have that

$$\begin{aligned} ||(\hat{\boldsymbol{\sigma}}, \boldsymbol{u})||_{\boldsymbol{H}} &\le ||(\boldsymbol{\sigma}, \boldsymbol{u})||_{\boldsymbol{H}} + ||(\widehat{\boldsymbol{\sigma}}_{\boldsymbol{g}}, \mathbf{0})||_{\boldsymbol{H}} \\ &\le C \left(||\boldsymbol{f}||_{[L^2(\Omega)]^2} + ||\boldsymbol{\zeta}||_{[L^2(\Omega)]^{2\times 2}} \right) + ||\widehat{\boldsymbol{\sigma}}_{\boldsymbol{g}}||_{[L^2(\Omega)]^{2\times 2}} \\ &\le C\, ||\boldsymbol{f}||_{[L^2(\Omega)]^2} + \tilde{C} \left(\frac{C}{2\,\mu} + 1 \right) ||\boldsymbol{g}||_{[H_{00}^{-1/2}(\Gamma_N)]^2} \,. \end{aligned}$$

□

Remark 17 *If* $(\boldsymbol{\sigma},\boldsymbol{u})$ *is the solution of* (43)-(44), *then* $\boldsymbol{\sigma}=\boldsymbol{\sigma}^{\mathtt{t}}$, $\boldsymbol{u}\in[H^1_{\Gamma_D}(\Omega)]^2$ *and* $\boldsymbol{\gamma}=\frac{\nabla\boldsymbol{u}-(\nabla\boldsymbol{u})^{\mathtt{t}}}{2}$.

As at the end of Section 2, we introduce a stabilized scheme of (43)-(44), such that the displacement is seeking in $[H^1_{\Gamma_D}(\Omega)]^2 := \{\boldsymbol{w}\in[H^1(\Omega)]^2 : \boldsymbol{w}=\mathbf{0} \quad \text{on} \quad \Gamma_D\}$. This lets us to get rid of $\boldsymbol{\gamma}$, as an independent unknown. As a consequence, we can consider the skew symmetric tensor $\boldsymbol{\gamma}(\boldsymbol{v}) := \frac{\nabla\boldsymbol{v}-(\nabla\boldsymbol{v})^{\mathtt{t}}}{2}$, for any $\boldsymbol{v}\in[H^1(\Omega)]^2$. Then, proceeding as in Section 3, we deduce the mixed variational formulation: *Find* $(\boldsymbol{\sigma},\boldsymbol{u})\in\tilde{H}_N\times[H^1_{\Gamma_D}(\Omega)]^2$ *such that*

$$\frac{1}{2\,\mu}\int_\Omega\boldsymbol{\sigma}^{\mathtt{d}} : \boldsymbol{\tau}^{\mathtt{d}} + \int_\Omega\boldsymbol{u}\cdot\mathbf{div}(\boldsymbol{\tau}) + \int_\Omega\gamma(\boldsymbol{u}) : \boldsymbol{\tau} = \int_\Omega\boldsymbol{\zeta} : \boldsymbol{\tau} \qquad \forall\,\boldsymbol{\tau}\in\tilde{H}_N\,, \tag{46}$$

$$-\int_\Omega\boldsymbol{v}\cdot\mathbf{div}(\boldsymbol{\sigma}) - \int_\Omega\gamma(\boldsymbol{v}) : \boldsymbol{\sigma} = \int_\Omega\boldsymbol{f}\cdot\boldsymbol{v} \qquad \forall\,\boldsymbol{v}\in[H^1_{\Gamma_D}(\Omega)]^2\,. \tag{47}$$

We also take into account the following least-square terms. For any $(\boldsymbol{\tau},\boldsymbol{v})\in H(\mathbf{div};\Omega)\times[H^1(\Omega)]^2$, we have

$$\kappa_1\int_\Omega\left(\boldsymbol{\varepsilon}(\boldsymbol{u}) - \frac{1}{2\,\mu}\boldsymbol{\sigma}^{\mathtt{d}}\right) : \left(\boldsymbol{\varepsilon}(\boldsymbol{v}) + \frac{1}{2\,\mu}\boldsymbol{\tau}^{\mathtt{d}}\right) = -\,\kappa_1\int_\Omega\boldsymbol{\zeta} : \left(\boldsymbol{\varepsilon}(\boldsymbol{v}) + \frac{1}{2\,\mu}\boldsymbol{\tau}^{\mathtt{d}}\right)\,, \tag{48}$$

$$\kappa_2\int_\Omega\mathbf{div}(\boldsymbol{\sigma})\cdot\mathbf{div}(\boldsymbol{\tau}) = -\,\kappa_2\int_\Omega\boldsymbol{f}\cdot\mathbf{div}(\boldsymbol{\tau})\,, \tag{49}$$

with $\kappa_1,\kappa_2\in\mathbb{R}$ at our disposal.

In what follows, we denote by $\tilde{\boldsymbol{H}} := \tilde{H}_N\times[H^1_{\Gamma_D}(\Omega)]^2 \subseteq \boldsymbol{H}$. We recall here that $\boldsymbol{H} := H(\mathbf{div};\Omega)\times[H^1(\Omega)]^2$, provided of its usual inner product and norm, as indicated in Section 3. Then, adding the equations (46), (47), (48), and (49), we obtain the augmented scheme: *Find* $(\boldsymbol{\sigma},\boldsymbol{u})\in\tilde{\boldsymbol{H}}$ *such that*

$$A_{\mathtt{s}}((\boldsymbol{\sigma},\boldsymbol{u}),(\boldsymbol{\tau},\boldsymbol{v})) = F_{\mathtt{s}}(\boldsymbol{\tau},\boldsymbol{v})\,, \quad \forall\,(\boldsymbol{\tau},\boldsymbol{v})\in\tilde{\boldsymbol{H}} \tag{50}$$

where the bilinear form $A_{\mathtt{s}} : \boldsymbol{H}\times\boldsymbol{H}\to\mathbb{R}$ is given by

$$\begin{aligned} A_{\mathtt{s}}((\boldsymbol{\rho},\boldsymbol{w}),(\boldsymbol{\tau},\boldsymbol{v})) := {} & \frac{1}{2\,\mu}\int_\Omega\boldsymbol{\rho}^{\mathtt{d}} : \boldsymbol{\tau}^{\mathtt{d}} + \int_\Omega\boldsymbol{w}\cdot\mathbf{div}(\boldsymbol{\tau}) + \int_\Omega\boldsymbol{\tau} : \gamma(\boldsymbol{w}) \\ & - \int_\Omega\boldsymbol{v}\cdot\mathbf{div}(\boldsymbol{\rho}) - \int_\Omega\boldsymbol{\rho} : \gamma(\boldsymbol{v}) + \kappa_1\int_\Omega\left(\boldsymbol{\varepsilon}(\boldsymbol{w}) - \frac{1}{2\,\mu}\boldsymbol{\rho}^{\mathtt{d}}\right) : \left(\boldsymbol{\varepsilon}(\boldsymbol{v}) + \frac{1}{2\,\mu}\boldsymbol{\tau}^{\mathtt{d}}\right) \\ & + \kappa_2\int_\Omega\mathbf{div}(\boldsymbol{\rho})\cdot\mathbf{div}(\boldsymbol{\tau}) \quad \forall\,(\boldsymbol{\rho},\boldsymbol{w}),(\boldsymbol{\tau},\boldsymbol{v})\in\boldsymbol{H}\,, \end{aligned}$$

and the linear functional $F_{\mathtt{s}} : \boldsymbol{H}\to\mathbb{R}$ is defined by

$$F_{\mathtt{s}}(\boldsymbol{\tau},\boldsymbol{v}) := \int_\Omega\boldsymbol{f}\cdot(\,\boldsymbol{v} - \kappa_2\,\mathbf{div}(\boldsymbol{\tau})\,) - \kappa_1\int_\Omega\boldsymbol{\zeta} : \left(\boldsymbol{\varepsilon}(\boldsymbol{v}) + \frac{1}{2\,\mu}\boldsymbol{\tau}^{\mathtt{d}}\right) + \int_\Omega\boldsymbol{\zeta} : \boldsymbol{\tau} \quad \forall\,(\boldsymbol{\tau},\boldsymbol{v})\in\boldsymbol{H}\,.$$

We now study for which values of κ_1 and κ_2, we can invoke Lax-Milgram theorem and ensure the unique solvability of (50). Lemma 15 and Korn's inequality in $[H^1_{\Gamma_D}(\Omega)]^2$ (cf. Chapter VI in [18]) will be useful to achieve this aim. As a result, it can be proved that when $\kappa_1\in(0,2\,\mu)$, and $\kappa_2>0$, bilinear form $A_{\mathtt{s}}$ is bounded in $\boldsymbol{H}$, and elliptic on $\tilde{\boldsymbol{H}}$. This means that there exist positive constants M and α, such that

$$\begin{aligned} |A_{\mathtt{s}}((\boldsymbol{\rho},\boldsymbol{w}),(\boldsymbol{\tau},\boldsymbol{v}))| \;&\leq\; M\,\|(\boldsymbol{\rho},\boldsymbol{w})\|_{\boldsymbol{H}}\,\|(\boldsymbol{\tau},\boldsymbol{v})\|_{\boldsymbol{H}}\,, \qquad \forall\,(\boldsymbol{\rho},\boldsymbol{w}),\,(\boldsymbol{\tau},\boldsymbol{v})\in\boldsymbol{H}\,,\\ A_{\mathtt{s}}((\boldsymbol{\tau},\boldsymbol{v}),(\boldsymbol{\tau},\boldsymbol{v})) \;&\geq\; \alpha\,\|(\boldsymbol{\tau},\boldsymbol{v})\|^2_{\boldsymbol{H}}\,, \qquad \forall\,(\boldsymbol{\tau},\boldsymbol{v})\;\in\;\tilde{\boldsymbol{H}}\,. \end{aligned}$$

By Lax-Milgram theorem, it is proved that the augmented variational formulation (50) has a unique solution $(\boldsymbol{\sigma},\boldsymbol{u})\in\tilde{\boldsymbol{H}}$, and there exists a positive constant C, such that

$$\|(\boldsymbol{\sigma},\boldsymbol{u})\|_{\boldsymbol{H}}\;\leq\;C\,\left(\|\boldsymbol{f}\|_{[L^2(\Omega)]^2}\;+\;||\boldsymbol{g}||_{[H_{00}^{-1/2}(\Gamma_N)]^2}\right)\,.$$

Now, for the discretization, we consider the same notations given in Sections 3 and 4. However, in this situation, we have $\mathcal{E}_h^{\partial}\;:=\;\mathcal{E}_h^{\mathtt{D}}\cup\mathcal{E}_h^{\mathtt{N}}$, with $\mathcal{E}_h^{\mathtt{D}}:=\{e\in\mathcal{E}_h^{\partial}\;:\;e\;\subset\;\Gamma_D\}$ and $\mathcal{E}_h^{\mathtt{N}},:=\{e\in\mathcal{E}_h^{\partial}\;:\;e\;\subset\;\Gamma_N\}$. As a consequence, given a triangulation $\mathcal{T}_h$ of $\overline{\Omega}$, its skeleton can be characterized as $\mathcal{E}_h\;=\;\mathcal{E}_h^{\mathtt{I}}\cup\mathcal{E}_h^{\mathtt{D}}\cup\mathcal{E}_h^{\mathtt{N}}$.

Now, in order to define the discrete variational formulation associated to problem (50), we first introduce the finite element subspaces:

$$\begin{aligned} H_h^{\boldsymbol{\sigma}}\;&:=\;\left\{\,\boldsymbol{\tau}_h\in H(\mathbf{div};\Omega)\;:\;\boldsymbol{\tau}_h|_T\;\in\;[\mathcal{RT}_\ell(T)^{\mathtt{t}}]^2\,,\quad\forall\,T\;\in\;\mathcal{T}_h\,\right\}\,,\\ H_{\mathtt{N},h}^{\boldsymbol{\sigma}}\;&:=\;\left\{\,\boldsymbol{\tau}_h\in H_h^{\boldsymbol{\sigma}}\;:\;\boldsymbol{\tau}_h\,\boldsymbol{\nu}\;=\;0\quad\text{on}\quad\mathcal{E}_h^{\mathtt{N}}\,\right\}\,,\\ H_h^{\boldsymbol{u}}\;&:=\;\left\{\,\boldsymbol{v}_h\;\in\;[\mathcal{C}(\overline{\Omega})]^2\;:\;\boldsymbol{v}_h|_T\;\in\;[\mathcal{P}_{\ell+1}(T)]^2\quad\forall\,T\;\in\;\mathcal{T}_h\quad\wedge\quad\boldsymbol{v}_h\;=\;0\quad\text{on}\quad\mathcal{E}_h^{\mathtt{D}}\right\}\,. \end{aligned}$$

Then, we propose the finite element subspace $\tilde{\boldsymbol{H}}_h\;:=\;H_{\mathtt{N},h}^{\boldsymbol{\sigma}}\times H_h^{\boldsymbol{u}}\;\subset\;\tilde{\boldsymbol{H}}$. As a result, we derive the conforming discrete variational formulation: *Find* $(\boldsymbol{\sigma}_h,\boldsymbol{u}_h)\;\in\;\tilde{\boldsymbol{H}}_h$ *such that*

$$A_{\mathtt{s}}((\boldsymbol{\sigma}_h,\boldsymbol{u}_h),(\boldsymbol{\tau}_h,\boldsymbol{v}_h))\;=\;F_{\mathtt{s}}(\boldsymbol{\tau}_h,\boldsymbol{v}_h)\qquad\forall\,(\boldsymbol{\tau}_h,\boldsymbol{v}_h)\in\tilde{\boldsymbol{H}}_h\,. \tag{51}$$

We remark that the Galerkin scheme (51) is well-posed and a Céa's estimate can be obtained. In addition, the corresponding rate of convergence of the Galerkin scheme (51) for this particular choice of finite element subspaces, is presented in the next theorem.

Theorem 18 *Let* $(\boldsymbol{\sigma},\boldsymbol{u})\in\tilde{\boldsymbol{H}}$ *and* $(\boldsymbol{\sigma}_h,\boldsymbol{u}_h)\in\tilde{\boldsymbol{H}}_h$ *be the unique solutions to problems* (50) *and* (51)*, respectively. In addition, assume that* $\boldsymbol{\sigma}\in[H^r(\Omega)]^{2\times2}$, $\mathbf{div}(\boldsymbol{\sigma})\in[H^r(\Omega)]^2$ *and* $\boldsymbol{u}\in[H^{r+1}(\Omega)]^2$ *for some* $r\in(0,\ell+1]$. *Then, there exists* $C>0$*, independent of* h*, such that there holds*

$$\|(\boldsymbol{\sigma},\boldsymbol{u})-(\boldsymbol{\sigma}_h,\boldsymbol{u}_h)\|_{\boldsymbol{H}}\;\leq\;C\,h^r\;\left(\|\boldsymbol{\sigma}\|_{[H^r(\Omega)]^{2\times2}}\;+\;\|\mathbf{div}(\boldsymbol{\sigma})\|_{[H^r(\Omega)]^2}\;+\;\|\boldsymbol{u}\|_{[H^{r+1}(\Omega)]^2}\right)\,.$$

Proof. It is a consequence of Céa's estimate, and the corresponding approximation properties. We omit further details. □

Remark 19 *We propose* $\hat{\boldsymbol{\sigma}}_h\;:=\;\boldsymbol{\sigma}_h\;+\;\boldsymbol{\varepsilon}(\boldsymbol{z}_h)$*, with* $\boldsymbol{z}_h\;\in\;H_h^{\boldsymbol{u}}$ *being the solution of discrete primal formulation associated to* (41)*. Then, assuming that* $\boldsymbol{z}\;\in\;[H^1_{\Gamma_D}(\Omega)\cap H^{s+1}(\Omega)]^2$*, for some* $s\in(0,\ell+1]$*, and invoking Theorem 18, we deduce*

$$\begin{aligned} &\|(\hat{\boldsymbol{\sigma}},\boldsymbol{u})-(\hat{\boldsymbol{\sigma}}_h,\boldsymbol{u}_h)\|_{\boldsymbol{H}}\\ &\leq\;C\left\{h^r\;\left(\|\boldsymbol{\sigma}\|_{[H^r(\Omega)]^{2\times2}}\;+\;\|\mathbf{div}(\boldsymbol{\sigma})\|_{[H^r(\Omega)]^2}\;+\;\|\boldsymbol{u}\|_{[H^{r+1}(\Omega)]^2}\right)\;+\;h^s\,||\boldsymbol{z}||_{[H^{s+1}(\Omega)]^2}\right\}\,. \end{aligned}$$

At this point, we remark that in general $\boldsymbol{\varepsilon}(\boldsymbol{z}_h)$ does not belong to $H^{\boldsymbol{\sigma}}_{\mathtt{N},h}$, and requires to know first $\boldsymbol{z}_h \in H^{\boldsymbol{u}}_h$ in order to calculate it. From a computational point of view, this could be expensive.

Reviewing [14], we propose a reasonable alternative. First, we introduce $\boldsymbol{g}_h := \pi^{\ell}_h(\boldsymbol{g})$ on $\mathcal{E}^{\mathtt{N}}_h$. Hereafter, $\pi^{\ell}_h(\boldsymbol{g})$ represents the L^2-orthogonal projection of $\boldsymbol{g}$ onto $\mathcal{P}_\ell(\mathcal{E}^{\mathtt{N}}_h)$. Proceeding as at the beginning of this Section, we ensure that there exists a unique solution $(\hat{\boldsymbol{\rho}}, \boldsymbol{w}, q)$ of problem (40), with traction $\boldsymbol{g}_h$ on Γ_N, that is

$$\begin{cases} \hat{\boldsymbol{\rho}} & = 2\,\mu\,\boldsymbol{\varepsilon}(\boldsymbol{w}) + q\,\boldsymbol{I} \quad \text{in} \quad \Omega\,, \\ -\,\mathbf{div}(\hat{\boldsymbol{\rho}}) & = \boldsymbol{f} \quad \text{in} \quad \Omega\,, \\ \operatorname{div}(\boldsymbol{w}) & = 0 \quad \text{in} \quad \Omega\,, \\ \boldsymbol{w} & = \boldsymbol{0} \quad \text{on} \quad \Gamma_D\,, \\ \hat{\boldsymbol{\rho}}\,\boldsymbol{\nu} & = \boldsymbol{g}_h \quad \text{on} \quad \Gamma_N\,. \end{cases} \tag{52}$$

Indeed, we deduce that $q = \frac{1}{2}\operatorname{tr}(\hat{\boldsymbol{\rho}})$.

This allows us to establish the existence and uniqueness of $(\boldsymbol{\rho}, \boldsymbol{w}) \in \tilde{\boldsymbol{H}}$ and $(\boldsymbol{\rho}_h, \boldsymbol{w}_h) \in \tilde{\boldsymbol{H}}_h$, solution of the analog problems (50) and (51), respectively. It is not difficult to check that

$$||(\hat{\boldsymbol{\sigma}} - \hat{\boldsymbol{\rho}}_h, \boldsymbol{u} - \boldsymbol{w}_h)||_{\boldsymbol{H}} \,\le\, ||(\hat{\boldsymbol{\sigma}} - \hat{\boldsymbol{\rho}}, \boldsymbol{u} - \boldsymbol{w})||_{\boldsymbol{H}} \,+\, ||(\hat{\boldsymbol{\rho}} - \hat{\boldsymbol{\rho}}_h, \boldsymbol{w} - \boldsymbol{w}_h)||_{\boldsymbol{H}}\,. \tag{53}$$

Now, applying similar arguments to the ones described in [14], and assuming in addition that $\boldsymbol{g} \in [L^2(\Gamma_N)]^2$, we can deduce that there exists $C > 0$, independent of h, such that

$$||(\hat{\boldsymbol{\sigma}} - \hat{\boldsymbol{\rho}}, \boldsymbol{u} - \boldsymbol{w})||_{\boldsymbol{H}} \,\le\, C\,\left(\sum_{T\in\mathcal{T}_h} \operatorname{osc}(\boldsymbol{g}, T)^2\right)^{1/2}\,, \tag{54}$$

where for each $T \in \mathcal{T}_h \,:\, |E(T) \cap \mathcal{E}^{\mathtt{N}}_h| \,>\, 0$

$$\operatorname{osc}(\boldsymbol{g}, T)^2 \,:=\, \sum_{e\,\in\,E(T)\,\cap\,\mathcal{E}^{\mathtt{N}}_h} h_e\,||\boldsymbol{g} \,-\, \pi^{\ell}_h(\boldsymbol{g})||^2_{[L^2(e)]^2}\,. \tag{55}$$

Now, invoking the *Raviart-Thomas local lifting operator on the normal trace* (cf. Proposition 2.4 in [26]), we can build $\tilde{\boldsymbol{\rho}}_{\boldsymbol{g}_h} \in H(\mathbf{div};\Omega) \cap [\mathcal{RT}_\ell(\mathcal{T}_h)]^2$, such that $\tilde{\boldsymbol{\rho}}_{\boldsymbol{g}_h}\,\boldsymbol{\nu} \,=\, \boldsymbol{g}_h$ on Γ_N. Here, we can not ensure the symmetry of $\tilde{\boldsymbol{\rho}}_{\boldsymbol{g}_h}$. Then, we consider $\hat{\boldsymbol{\rho}} \,=\, \tilde{\boldsymbol{\rho}} \,+\, \tilde{\boldsymbol{\rho}}_{\boldsymbol{g}_h}$ in Ω, with $\tilde{\boldsymbol{\rho}}\,\boldsymbol{\nu} \,=\, \boldsymbol{0}$ on Γ_N. This helps us to rewrite (40) as:

$$\begin{cases} -\,\mathbf{div}(\tilde{\boldsymbol{\rho}}) & = \tilde{\boldsymbol{f}} \quad \text{in} \quad \Omega\,, \\ \frac{1}{2\,\mu}\,\tilde{\boldsymbol{\rho}}^{\mathtt{d}} & = \boldsymbol{\nabla}\boldsymbol{w} \,-\, \gamma(\boldsymbol{w}) \,+\, \tilde{\boldsymbol{\zeta}} \quad \text{in} \quad \Omega\,, \\ \operatorname{div}(\boldsymbol{w}) & = 0 \quad \text{in} \quad \Omega\,, \\ \boldsymbol{w} & = \boldsymbol{0} \quad \text{on} \quad \Gamma_D\,, \\ \tilde{\boldsymbol{\rho}}\,\boldsymbol{\nu} & = \boldsymbol{0} \quad \text{on} \quad \Gamma_N\,, \end{cases} \tag{56}$$

where $\tilde{\boldsymbol{f}} := \boldsymbol{f} + \mathbf{div}(\tilde{\boldsymbol{\rho}}_{\boldsymbol{g}_h})$, and $\tilde{\boldsymbol{\zeta}} := -\frac{1}{2\mu}\tilde{\boldsymbol{\rho}}^{\mathtt{d}}_{\boldsymbol{g}_h}$. We notice that the hydrostatic pressure is recovered from $q = \frac{1}{2}\mathrm{tr}(\hat{\boldsymbol{\rho}})$.

We emphasize that $(\tilde{\boldsymbol{\rho}}, \boldsymbol{w}) \in \tilde{\boldsymbol{H}}$ and $(\tilde{\boldsymbol{\rho}}_h, \boldsymbol{w}_h) \in \tilde{\boldsymbol{H}}_h$ satisfy

$$\forall\,(\boldsymbol{\tau}, \boldsymbol{v}) \in \tilde{\boldsymbol{H}} \,:\, A_{\mathtt{s}}((\tilde{\boldsymbol{\rho}}, \boldsymbol{w}), (\boldsymbol{\tau}, \boldsymbol{v})) = \tilde{F}_{\mathtt{s}}(\boldsymbol{\tau}, \boldsymbol{v})\,, \tag{57}$$

$$\forall\,(\boldsymbol{\tau}, \boldsymbol{v}) \in \tilde{\boldsymbol{H}}_h \,:\, A_{\mathtt{s}}((\tilde{\boldsymbol{\rho}}_h, \boldsymbol{w}_h), (\boldsymbol{\tau}, \boldsymbol{v})) = \tilde{F}_{\mathtt{s}}(\boldsymbol{\tau}, \boldsymbol{v})\,, \tag{58}$$

respectively, with $\tilde{F}_{\mathtt{s}} : \boldsymbol{H} \to \mathbb{R}$ being the linear functional, given for any $(\boldsymbol{\tau}, \boldsymbol{v}) \in \boldsymbol{H}$, by

$$\tilde{F}_{\mathtt{s}}(\boldsymbol{\tau}, \boldsymbol{v}) := \int_\Omega \tilde{\boldsymbol{f}} \cdot (\boldsymbol{v} - \kappa_2\,\mathbf{div}(\boldsymbol{\tau})) - \kappa_1 \int_\Omega \tilde{\boldsymbol{\zeta}} : \left(\boldsymbol{\varepsilon}(\boldsymbol{v}) + \frac{1}{2\,\mu}\boldsymbol{\tau}^{\mathtt{d}}\right) + \int_\Omega \tilde{\boldsymbol{\zeta}} : \boldsymbol{\tau} + \int_\Omega \tilde{\boldsymbol{\rho}}_{\boldsymbol{g}_h} : \boldsymbol{\gamma}(\boldsymbol{v})\,.$$

Remark 20 *$\hat{\boldsymbol{\rho}}_h := \tilde{\boldsymbol{\rho}}_h + \tilde{\boldsymbol{\rho}}_{\boldsymbol{g}_h} \in H_h^{\boldsymbol{\sigma}}$ results to be a suitable approximation of $\hat{\boldsymbol{\rho}} := \tilde{\boldsymbol{\rho}} + \tilde{\boldsymbol{\rho}}_{\boldsymbol{g}_h}$. Moreover, since $\hat{\boldsymbol{\rho}} - \hat{\boldsymbol{\rho}}_h = \tilde{\boldsymbol{\rho}} - \tilde{\boldsymbol{\rho}}_h$, and according to Theorem 18, we expect convergence at the same rate, at least.*

6 An a posteriori error estimator

In this section, we derive an a posteriori error estimate to (58), which results to be reliable and locally efficient. We follow similar ideas to the given in Section 4. However, since we are dealing with an equivalent problem with homogeneous mixed boundary conditions, we do not require to introduce the Ritz projection of the error, nor performing any quasi-Helmholtz decomposition of functions in $H(\mathbf{div};\Omega)$, as we have done in Section 4.

Let $(\tilde{\boldsymbol{\rho}}, \boldsymbol{w}) \in \tilde{\boldsymbol{H}}$ and $(\tilde{\boldsymbol{\rho}}_h, \boldsymbol{w}_h) \in \tilde{\boldsymbol{H}}_h$ be the unique solution of problems (57) and (58), respectively. Since $\tilde{\boldsymbol{H}}_h \subset \tilde{\boldsymbol{H}}$, we have the orthogonality relation

$$A_{\mathtt{s}}((\tilde{\boldsymbol{\rho}} - \tilde{\boldsymbol{\rho}}_h, \boldsymbol{w} - \boldsymbol{w}_h), (\boldsymbol{\tau}, \boldsymbol{v})) = 0 \quad \forall\,(\boldsymbol{\tau}, \boldsymbol{v}) \in \tilde{\boldsymbol{H}}_h\,. \tag{59}$$

On the other hand, using the strong coercivity of $A_{\mathtt{s}}$ on $\tilde{\boldsymbol{H}}$, we are able to establish

$$\alpha\,||(\tilde{\boldsymbol{\rho}} - \tilde{\boldsymbol{\rho}}_h, \boldsymbol{w} - \boldsymbol{w}_h)||_{\boldsymbol{H}} \le \sup_{(\boldsymbol{\tau},\boldsymbol{v})\in\tilde{\boldsymbol{H}}\setminus\{(\mathbf{0},\mathbf{0})\}} \frac{A_{\mathtt{s}}((\tilde{\boldsymbol{\rho}} - \tilde{\boldsymbol{\rho}}_h, \boldsymbol{w} - \boldsymbol{w}_h), (\boldsymbol{\tau}, \boldsymbol{v}))}{||(\boldsymbol{\tau}, \boldsymbol{v})||_{\boldsymbol{H}}}\,. \tag{60}$$

Then, according to (60), and with the purpose of obtaining a reliable a posteriori error estimator for the discrete scheme (58), it is enough to bound from above the supremum in (60).

To this aim, we first establish the following result.

Lemma 21 *For any $(\boldsymbol{\tau}, \boldsymbol{v}) \in \tilde{\boldsymbol{H}}$, there holds*

$$A_{\mathtt{s}}((\tilde{\boldsymbol{\rho}} - \tilde{\boldsymbol{\rho}}_h, \boldsymbol{w} - \boldsymbol{w}_h), (\boldsymbol{\tau}, \boldsymbol{v})) = S_1(\boldsymbol{\tau}) + S_2(\boldsymbol{v})\,,$$

where

$$S_1(\boldsymbol{\tau}) \;:=\; \int_\Omega \left(\tilde{\boldsymbol{\zeta}} + \boldsymbol{\varepsilon}(\boldsymbol{w}_h) - \frac{1}{2\,\mu}\tilde{\boldsymbol{\rho}}_h^{\mathtt{d}}\right) \,:\, \boldsymbol{\tau} \;-\; \frac{\kappa_1}{2\,\mu}\int_\Omega \left(\tilde{\boldsymbol{\zeta}} + \boldsymbol{\varepsilon}(\boldsymbol{w}_h) - \frac{1}{2\,\mu}\tilde{\boldsymbol{\rho}}_h^{\mathtt{d}}\right) \,:\, \boldsymbol{\tau}^{\mathtt{d}}$$
$$-\; \kappa_2 \int_\Omega \left(\tilde{\boldsymbol{f}} + \mathbf{div}(\tilde{\boldsymbol{\rho}}_h)\right) \cdot \mathbf{div}(\boldsymbol{\tau})\,, \tag{61}$$

$$S_2(\boldsymbol{v}) \;:=\; \int_\Omega \left(\tilde{\boldsymbol{f}} + \mathbf{div}(\tilde{\boldsymbol{\rho}}_h)\right) \cdot \boldsymbol{v} \;-\; \kappa_1 \int_\Omega \left(\tilde{\boldsymbol{\zeta}} + \boldsymbol{\varepsilon}(\boldsymbol{w}_h) - \frac{1}{2\,\mu}\tilde{\boldsymbol{\rho}}_h^{\mathtt{d}}\right) \,:\, \boldsymbol{\varepsilon}(\boldsymbol{v})$$
$$+\; \frac{1}{2}\int_\Omega \left[(\tilde{\boldsymbol{\rho}}_h + \tilde{\boldsymbol{\rho}}_{\boldsymbol{g}_h}) - (\tilde{\boldsymbol{\rho}}_h + \tilde{\boldsymbol{\rho}}_{\boldsymbol{g}_h})^{\mathtt{t}}\right] \,:\, \boldsymbol{\gamma}(\boldsymbol{v})\,. \tag{62}$$

Proof. The proof relies on integrating by parts $\displaystyle\int_\Omega \boldsymbol{w}_h \cdot \mathbf{div}(\boldsymbol{\tau})$, performing algebraic manipulations and invoking Cauchy-Schwarz inequality. We omit further details. $\square$

Next, after applying Cauchy-Schwarz inequality, and invoking (35), (36), we can bound functionals S_1 and S_2. In order to clarify the presentation, we collect these results in the following lemmas.

Lemma 22 *For any $\boldsymbol{\tau} \in \tilde{H}_N$, there holds*

$$|S_1(\boldsymbol{\tau})| \;\leq\; \left(\left\|\tilde{\boldsymbol{\zeta}} + \boldsymbol{\varepsilon}(\boldsymbol{w}_h) - \frac{1}{2\,\mu}\tilde{\boldsymbol{\rho}}_h^{\mathtt{d}}\right\|_{[L^2(\Omega)]^{2\times 2}} \;+\; \kappa_2\,||\tilde{\boldsymbol{f}} + \mathbf{div}(\tilde{\boldsymbol{\rho}}_h)||_{[L^2(\Omega)]^2} \right) \,||\boldsymbol{\tau}||_{H(\mathbf{div};\Omega)}\,. \tag{63}$$

Lemma 23 *For any $\boldsymbol{v} \in [H^1_{\Gamma_D}(\Omega)]^2$ there holds*

$$|S_2(\boldsymbol{v})| \;\leq\; \Bigg(||\tilde{\boldsymbol{f}} + \mathbf{div}(\tilde{\boldsymbol{\rho}}_h)||_{[L^2(\Omega)]^2} \;+\; \kappa_1 \left\|\tilde{\boldsymbol{\zeta}} + \boldsymbol{\varepsilon}(\boldsymbol{w}_h) - \frac{1}{2\,\mu}\tilde{\boldsymbol{\rho}}_h^{\mathtt{d}}\right\|_{[L^2(\Omega)]^{2\times 2}}$$
$$+\,\frac{1}{2}\left\|(\tilde{\boldsymbol{\rho}}_h + \tilde{\boldsymbol{\rho}}_{\boldsymbol{g}_h}) - (\tilde{\boldsymbol{\rho}}_h + \tilde{\boldsymbol{\rho}}_{\boldsymbol{g}_h})^{\mathtt{t}}\right\|_{[L^2(\Omega)]^{2\times 2}} \Bigg) \,||\boldsymbol{v}||_{[H^1(\Omega)]^2}\,. \tag{64}$$

As a result, we obtain a reliable residual a posteriori error estimator, which is established in the following result.

Theorem 24 *There exists $C_{\mathtt{rel}} > 0$, independent of h, such that*

$$C_{\mathtt{rel}}\,||(\tilde{\boldsymbol{\rho}} - \tilde{\boldsymbol{\rho}}_h, \boldsymbol{w} - \boldsymbol{w}_h)||_{\boldsymbol{H}} \;\leq\; \eta \;:=\; \left(\sum_{T\in\mathcal{T}_h} \eta_T^2\right)^{1/2}\,, \tag{65}$$

where for any $T \in \mathcal{T}_h$

$$\eta_T^2 \;:=\; \max\{1,\kappa_1^2\} \left\|\tilde{\boldsymbol{\zeta}} + \boldsymbol{\varepsilon}(\boldsymbol{w}_h) - \frac{1}{2\,\mu}\tilde{\boldsymbol{\rho}}_h^{\mathtt{d}}\right\|^2_{[L^2(T)]^{2\times 2}} \;+\; \max\{1,\kappa_2^2\}\,||\tilde{\boldsymbol{f}} + \mathbf{div}(\tilde{\boldsymbol{\rho}}_h)||^2_{[L^2(T)]^2}$$
$$+\; \frac{1}{4}\,\left\|(\tilde{\boldsymbol{\rho}}_h + \tilde{\boldsymbol{\rho}}_{\boldsymbol{g}_h}) - (\tilde{\boldsymbol{\rho}}_h + \tilde{\boldsymbol{\rho}}_{\boldsymbol{g}_h})^{\mathtt{t}}\right\|^2_{[L^2(T)]^{2\times 2}}\,. \tag{66}$$

Proof. It follows from Lemmas 22 and 23. We omit further details. □

Now, for any $T \in \mathcal{T}_h$, we notice that

$$\begin{aligned}
\tilde{\boldsymbol{\zeta}} + \boldsymbol{\varepsilon}(\boldsymbol{w}_h) - \frac{1}{2\,\mu}\tilde{\boldsymbol{\rho}}_h^{\mathtt{d}} \,&=\, \frac{1}{2\,\mu}\,\tilde{\boldsymbol{\rho}}^{\mathtt{d}} \,-\, \boldsymbol{\varepsilon}(\boldsymbol{w}) + \boldsymbol{\varepsilon}(\boldsymbol{w}_h) - \frac{1}{2\,\mu}\tilde{\boldsymbol{\rho}}_h^{\mathtt{d}} \,=\, \frac{1}{2\,\mu}\,(\tilde{\boldsymbol{\rho}} - \tilde{\boldsymbol{\rho}}_h)^{\mathtt{d}} \,+\, \boldsymbol{\varepsilon}(\boldsymbol{w}_h - \boldsymbol{w})\,, \\
\tilde{\boldsymbol{f}} + \mathbf{div}(\tilde{\boldsymbol{\rho}}_h) \,&=\, \mathbf{div}(\tilde{\boldsymbol{\rho}}_h - \tilde{\boldsymbol{\rho}})\,, \\
(\tilde{\boldsymbol{\rho}}_h + \tilde{\boldsymbol{\rho}}_{\boldsymbol{g}_h}) - (\tilde{\boldsymbol{\rho}}_h + \tilde{\boldsymbol{\rho}}_{\boldsymbol{g}_h})^{\mathtt{t}} \,&=\, (\tilde{\boldsymbol{\rho}}_h + \tilde{\boldsymbol{\rho}}_{\boldsymbol{g}_h}) - (\tilde{\boldsymbol{\rho}}_h + \tilde{\boldsymbol{\rho}}_{\boldsymbol{g}_h})^{\mathtt{t}} \,-\, (\tilde{\boldsymbol{\rho}} + \tilde{\boldsymbol{\rho}}_{\boldsymbol{g}_h}) + (\tilde{\boldsymbol{\rho}} + \tilde{\boldsymbol{\rho}}_{\boldsymbol{g}_h})^{\mathtt{t}} \,=\, (\tilde{\boldsymbol{\rho}}_h - \tilde{\boldsymbol{\rho}}) \,-\, (\tilde{\boldsymbol{\rho}}_h - \tilde{\boldsymbol{\rho}})^{\mathtt{t}}\,.
\end{aligned}$$

As a consequence, after invoking Minkowski inequality and algebraic manipulations, we deduce the following result, which establishes the local efficiency of our estimator.

Theorem 25 *There exists $C_{\mathtt{eff}} > 0$, independent of h, such that for any $T \in \mathcal{T}_h$ there holds*

$$\eta_T \,\leq C_{\mathtt{eff}}\, \max\{1, \kappa_1, \kappa_2\} \left(\max\left\{ \frac{1}{2\,\mu}, 1 \right\} \,||\tilde{\boldsymbol{\rho}} - \tilde{\boldsymbol{\rho}}_h||_{H(\mathbf{div};T)} \,+\, ||\boldsymbol{w} - \boldsymbol{w}_h||_{[H^1(T)]^2} \right)\,. \tag{67}$$

As a consequence, we can establish a reliable residual a posteriori error estimator for problem (40).

Theorem 26 *There exists $\tilde{C}_{\mathtt{rel}} > 0$, independent of h, such that*

$$\tilde{C}_{\mathtt{rel}}\, ||(\hat{\boldsymbol{\sigma}} - \hat{\boldsymbol{\rho}}_h, \boldsymbol{u} - \boldsymbol{w}_h)||_{\boldsymbol{H}} \,\leq \eta \,+\, \operatorname{osc}(\boldsymbol{g}; \mathcal{E}_h^{\mathtt{N}})\,, \tag{68}$$

where

$$\operatorname{osc}(\boldsymbol{g}; \mathcal{E}_h^{\mathtt{N}}) \,:=\, \left(\sum_{\substack{T\in\mathcal{T}_h \\ |E(T)\cap\mathcal{E}_h^{\mathtt{N}}|\neq 0}} \operatorname{osc}(\boldsymbol{g}, T)^2 \right)^{1/2}\,,$$

and for any $T \in \mathcal{T}_h \,:\, |E(T) \cap \mathcal{E}_h^{\mathtt{N}}| > 0$, $\operatorname{osc}(\boldsymbol{g}, T)$ is given by (55).

Proof. It relies on taking into account (54) and (65) to conclude from (53). We omit further details. □

Remark 27 *The oscillation term $\operatorname{osc}(\boldsymbol{g}; \mathcal{E}_h^{\mathtt{N}})$ could be seen as a high order term when $\boldsymbol{g}$ is smooth enough. For example, considering the lowest order of approximation (when $\ell = 0$), if $\boldsymbol{g} \in [H^1(\mathcal{E}_h^{\mathtt{N}})]^2$, then we deduce that $\operatorname{osc}(\boldsymbol{g}; \mathcal{E}_h^{\mathtt{N}}) = \mathcal{O}(h^{3/2})$. Thus, the oscillation term results to be a high order term.*

Remark 28 *When $\boldsymbol{g}$ is piecewise polynomial on Γ_N, there is no oscillation term. Therefore, invoking Theorems 24 and 25, we conclude that η is a reliable and locally efficient a posteriori error estimator for our problem.*

7 Numerical experiments

In this section, we present several numerical examples that exhibit the reliability and (local) efficiency of the proposed a posteriori error estimator (on each case: pure Dirichlet or mixed boundary conditions), when is applied a well known adaptive algorithm to improve the quality of approximation of the solution. In both situations, we consider the finite element subspaces of lowest order of approximation (i.e. for $\ell = 0$). As usual, we introduce some notations for the individual errors of each unknown. These ones are then define as

$$\boldsymbol{e}(\boldsymbol{\sigma}) := ||\boldsymbol{\sigma} - \boldsymbol{\sigma}_h||_{H(\mathbf{div};\Omega)}, \quad \boldsymbol{e}(\boldsymbol{u}) := ||\boldsymbol{u} - \boldsymbol{u}_h||_{[H^1(\Omega)]^2} \quad \text{and} \quad \boldsymbol{e} = \big(\boldsymbol{e}(\boldsymbol{\sigma})^2 + \boldsymbol{e}(\boldsymbol{u})^2\big)^{1/2}.$$

We set the effectivity index as $\boldsymbol{e}/\eta$. We recall that, if $\boldsymbol{e}$ and $\tilde{\boldsymbol{e}}$ stand for the errors at two consecutive triangulations wirh N and $\tilde{N}$ degrees of freedom, respectively, then the experimental rate of convergence is given by $r := -2\frac{\log(\boldsymbol{e}/\tilde{\boldsymbol{e}})}{\log(N/\tilde{N})}$. The definitions of $r(\boldsymbol{u})$, $r(\boldsymbol{\sigma})$ are given analogously.

The adaptive refinement algorithm we consider can be found in [36], and reads as follows:

Algorithm 1: Adaptive Refinement Algorithm

Result: Improvement of quality of approximation
Input: tolerance `tol`, initial / coarse mesh $\mathcal{T}_h^0$;
`Step 1:` Solve the Galerkin scheme for the current mesh $\mathcal{T}_h^0$. Then compute $\{\eta_T\}_{T\in\mathcal{T}_h^0}$.
while $\eta >$ `tol` **do**

`Mark each element` $T' \in \mathcal{T}_h$ `such that`

$$\eta_{T'} \geq \frac{1}{2}\max\{\eta_T : T \in \mathcal{T}_h\}.$$

`Refine marked elements and remove hanging nodes if corresponds`;
`This generates an adapted mesh` $\mathcal{T}_h$;
$\mathcal{T}_h^0 \leftarrow \mathcal{T}_h$ `and go to Step 1.`

end

7.1 A pure Dirichlet boundary condition problem with non smooth solution

In this case, we notice that the approximation space for $\boldsymbol{\sigma}$ includes a null mean value of the trace of its elements. This restriction on the stress tensor is weakly imposed in the discrete formulation with the help of a Lagrange multiplier, as in [10] (see also [29, 30]). More precisely, we solve the following auxiliary discrete scheme: *Find* $(\boldsymbol{\sigma}_h, \boldsymbol{u}_h, \varphi_h) \in \hat{\boldsymbol{H}}_h := H_h^{\boldsymbol{\sigma}} \times H_h^{\boldsymbol{u}} \times \mathbb{R}$ *such that*

$$\begin{aligned} A((\boldsymbol{\sigma}_h, \boldsymbol{u}_h), (\boldsymbol{\tau}_h, \boldsymbol{v}_h)) + \varphi_h \int_\Omega \mathrm{tr}(\boldsymbol{\tau}_h) &= F(\boldsymbol{\tau}_h, \boldsymbol{v}_h), \\ \psi_h \int_\Omega \mathrm{tr}(\boldsymbol{\sigma}_h) &= 0, \end{aligned} \tag{69}$$

for all $(\boldsymbol{\tau}_h, \boldsymbol{v}_h, \psi_h) \in \hat{\boldsymbol{H}}_h$. A standard argument establishes the equivalence between the variational problems (17) and (69). We refer to Theorem 6.1 in [12] for further details.

In what follows, DOF stands for the total number of degrees of freedom (unknowns) of (69), that is, $DOF = 2\times$(Numbers of vertexes of $\mathcal{T}_h$) + $2\times$ (Number of edges $\mathcal{T}_h$) +1, which leads asymptotically to 4 unknowns per triangle, which reflects the low computational cost, almost the same than the required by considering the $\mathcal{P}_1-$iso$\mathcal{P}_1$ elements for the standard velocity-pressure formulation, whose degrees of freedom are asymptotically 4.5 (unknowns) per triangle. In addition, by setting $p_h := -\frac{1}{2}\mathrm{tr}(\boldsymbol{\sigma}_h)$, we obtain a reasonable piecewise-linear approximation of the pressure $p = -\frac{1}{2}\mathrm{tr}(\boldsymbol{\sigma})$.

Our example is defined in the domain $\Omega := \{(x_1, x_2) \in \mathbb{R}^2 : x_1 , x_2 > 0 , x_1 + x_2 < 1\}$, and the corresponding data are taken so that the exact solution is

$$\boldsymbol{u}(x_1, x_2) := 10^2 \,\mathbf{curl}\left(\frac{x_1^2 x_2^2 (1 - x_1 - x_2)^2}{(x_1^2 + x_2^2)^{3/4}}\right), \quad p(x_1, x_2) := x_1^2 + x_2^2 - \frac{1}{3}.$$

We notice that $\boldsymbol{u}$ has a singularity at $(0, 0)$. Thus, the corresponding rate of convergence, when an uniform refinement algorithm is performed, should be below 1. We take $\mu = 1$, and chose $(\kappa_1, \kappa_2, \kappa_3) := (1, 1/2, 1/2)$, to ensure that the (17) has a unique solution.

From Table 1 we realize that the experimental rate of convergence of total error ($\boldsymbol{e}$), on uniform refinement, is close to 0.45 On the other side, the numerical results corresponding to the adaptive refinement Algorithm 1, based on η (which is given in Theorem 13), almost shows that the total error behaves as $\mathcal{O}(N^{-1/2})$ These two behaviour are displayed in Figure 1. In addition, the last column in Table 1 shows us that the efficiency index is close to 1, when uniform and adaptive refinement algorithms are performed. Some adaptive refined meshes are displayed in Figure 2, and exhibit the capability of the a posteriori error estimator η to localize the singularity at origin.

7.2 A benchmark problem with mixed boundary conditions having a non smooth solution

In this case, the problem has been taken from [36], where the displacement as well as the hydrostatic pressure are defined in $\Omega := \{(x_1, x_2) \in \mathbb{R}^2 : x_1^2 + x_2^2 < 1\} \setminus [0, 1] \times [-1, 0]$. The boundary $\Gamma := \partial\Omega$ is decomposed as $\Gamma = \Gamma_D \cup \Gamma_N$, with $\Gamma_D := \{0\} \times [-1, 0] \cup [0, 1] \times \{0\}$. We notice that the data of this problem are given such that the exact solution, in polar coordinates (r, θ), is

$$\boldsymbol{u}(r, \theta) := \begin{pmatrix} r^\lambda[(1 + \lambda) \sin(\theta)\, \psi(\theta) + \cos(\theta)\, \psi'(\theta)] \\ r^\lambda[-(1 + \lambda) \cos(\theta)\, \psi(\theta) + \sin(\theta)\, \psi'(\theta)] \end{pmatrix}, \quad \text{and}$$

$$p(r, \theta) := -\frac{r^{\lambda-1}}{1 - \lambda}[(1 + \lambda)^2 \psi'(\theta) + \psi'''(\theta)],$$

dof	$\boldsymbol{e}(\boldsymbol{u})$	$r(\boldsymbol{u})$	$\boldsymbol{e}(\boldsymbol{\sigma})$	$r(\boldsymbol{\sigma})$	$\boldsymbol{e}$	r	$\boldsymbol{e}/\eta$
91	0.130e+2	—-	0.153e+3	—-	0.154e+3	—-	0.9991
307	0.796e+1	0.8009	0.105e+3	0.6290	0.105e+3	0.6301	1.0001
1123	0.417e+1	0.9952	0.774e+2	0.4641	0.775e+2	0.4663	1.0004
4291	0.212e+1	1.0142	0.583e+2	0.4218	0.584e+2	0.4230	1.0002
16771	0.106e+1	1.0093	0.434e+2	0.4341	0.434e+2	0.4346	1.0001
66307	0.533e+0	1.0047	0.318e+2	0.4546	0.318e+2	0.4548	1.0001
dof	$\boldsymbol{e}(\boldsymbol{u})$	$r(\boldsymbol{u})$	$\boldsymbol{e}(\boldsymbol{\sigma})$	$r(\boldsymbol{\sigma})$	$\boldsymbol{e}$	r	$\boldsymbol{e}/\eta$
91	0.130e+2	—-	0.153e+3	—-	0.154e+3	—-	0.9991
143	0.104e+2	0.9601	0.120e+3	1.0779	0.121e+3	1.0770	0.9998
195	0.984e+1	0.3724	0.106e+3	0.8075	0.106e+3	0.8040	0.9992
331	0.917e+1	0.2653	0.871e+2	0.7431	0.876e+2	0.7385	0.9957
483	0.739e+1	1.1423	0.735e+2	0.8981	0.739e+2	0.9007	0.9974
535	0.739e+1	0.0065	0.707e+2	0.7706	0.711e+2	0.7626	0.9971
983	0.603e+1	0.6666	0.563e+2	0.7484	0.566e+2	0.7474	0.9975
1371	0.540e+1	0.6725	0.484e+2	0.9066	0.487e+2	0.9039	0.9982
2023	0.387e+1	1.7023	0.399e+2	0.9954	0.401e+2	1.0030	0.9994
2687	0.379e+1	0.1519	0.347e+2	0.9837	0.349e+2	0.9749	0.9988
3979	0.329e+1	0.7287	0.297e+2	0.7975	0.298e+2	0.7966	0.9981
6107	0.268e+1	0.9596	0.243e+2	0.9353	0.244e+2	0.9356	0.9973
8875	0.206e+1	1.3985	0.202e+2	0.9721	0.203e+2	0.9769	0.9980
11379	0.195e+1	0.4254	0.181e+2	0.9171	0.182e+2	0.9118	0.9978
16719	0.170e+1	0.7191	0.153e+2	0.8573	0.154e+2	0.8556	0.9976
24687	0.138e+1	1.0581	0.127e+2	0.9502	0.128e+2	0.9515	0.9983
36271	0.108e+1	1.2693	0.105e+2	1.0183	0.105e+2	1.0211	0.9982
46139	0.101e+1	0.5973	0.933e+1	0.9487	0.939e+1	0.9448	0.9984
68775	0.855e+0	0.8315	0.780e+1	0.8987	0.785e+1	0.8979	0.9988

Table 1: History of convergence and corresponding rates of convergence, Example 7.1, with $\mu = 1.0$ (uniform and adaptive refinements)

with

$$\psi(\theta) := \frac{1}{1+\lambda}\sin((1+\lambda)\theta)\cos(\lambda\,\omega) - \cos((1+\lambda)\theta) - \frac{1}{1-\lambda}\sin((1-\lambda)\theta)\cos(\lambda\,\omega) + \cos((1-\lambda)\theta)\,,$$

$$\lambda := 0.54448373678246\,, \quad \omega := \frac{3}{2}\pi\,.$$

In this case the exact solution $(\boldsymbol{u}, p)$ lives in $[H^{1+\lambda}(\Omega)]^2 \times H^{\lambda}(\Omega)$. Here, we also consider $\mu = 1$, which allows us to set $\kappa_1 := 1$. In addition, we choose $\kappa_2 := 1$. We notice that $\boldsymbol{u} = \mathbf{0}$ on Γ_D. On the other hand, the corresponding traction datum $\boldsymbol{g}$ is not piecewise polynomial on Γ_N. With the aim of obtaining an approximation of the problem with a non expensive cost, we take into account the

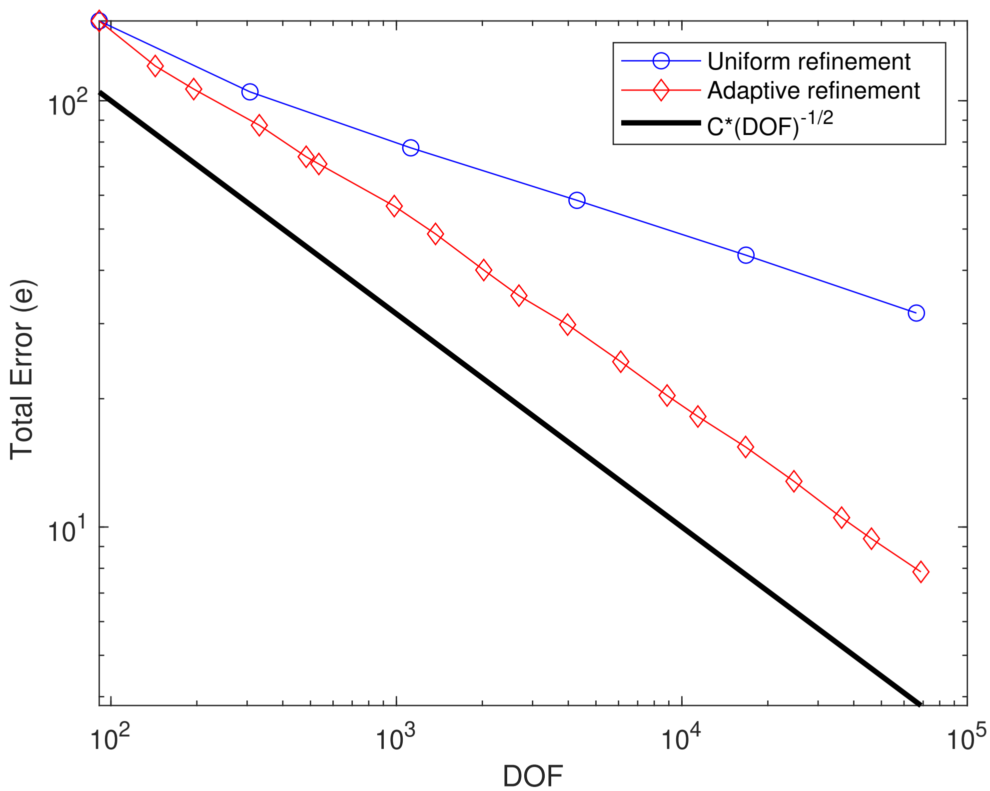

Figure 1: Total error ($\boldsymbol{e}$) vs DOF (N) for uniform and adaptive refinements (Example 7.1, with $\mu = 1.0$)

discussion given in Sections 5 and 6. Then, we consider the problem (52), where $\boldsymbol{g}_h$ represents the corresponding L^2-orthogonal projection of $\boldsymbol{g}$ onto $[\mathcal{P}_0(\mathcal{E}_h^{\mathtt{N}})]^2$.

Now, we point out that Proposition 2.4 in [26] gives us an strategy to construct $\tilde{\boldsymbol{\rho}}_{\boldsymbol{g}_h}$ (and then solve (58)) for the lowest order $\ell = 0$, that is $\tilde{\boldsymbol{\rho}}_{\boldsymbol{g}_h} \in H(\mathbf{div};\Omega) \cap [\mathcal{RT}_0(\mathcal{T}_h)]^2$. First, we set $\widetilde{\mathcal{T}}_{N,h} := \cup\{T \in \mathcal{T}_h : |\partial T \cap \mathcal{E}_h^{\mathtt{N}}| \neq 0\}$. Then we set $\tilde{\boldsymbol{\rho}}_{\boldsymbol{g}_h} := \mathbf{0}$ in $\mathcal{T}_h \backslash \widetilde{\mathcal{T}}_{N,h}$. For each $T \in \widetilde{\mathcal{T}}_{N,h}$, knowing that $\tilde{\boldsymbol{\rho}}_{\boldsymbol{g}_h}|_T \in [\mathcal{RT}_0(T)]^2$, it will be characterized by

$$\tilde{\boldsymbol{\rho}}_{\boldsymbol{g}_h} \boldsymbol{\nu} = \mathbf{0} \quad \text{on} \quad \partial T \backslash \mathcal{E}_h^{\mathtt{N}} \quad \text{and} \quad \tilde{\boldsymbol{\rho}}_{\boldsymbol{g}_h} \boldsymbol{\nu} = \boldsymbol{g}_h \quad \text{on} \quad \partial T \cap \mathcal{E}_h^{\mathtt{N}}.$$

We recall that Theorem 26, gives us an a posteriori error estimator (η), which will be used in Algorithm 1 to improve the quality of the exact solution. Then, we compute $\{\eta_T\}_{T\in\mathcal{T}_h}$ to perform our *Adaptive Refinement* procedure.

We display in Table 2 the history of convergence of the method, for sequences of uniform and adaptive refined meshes generated according to the proposed Algorithm 1. We observe that when

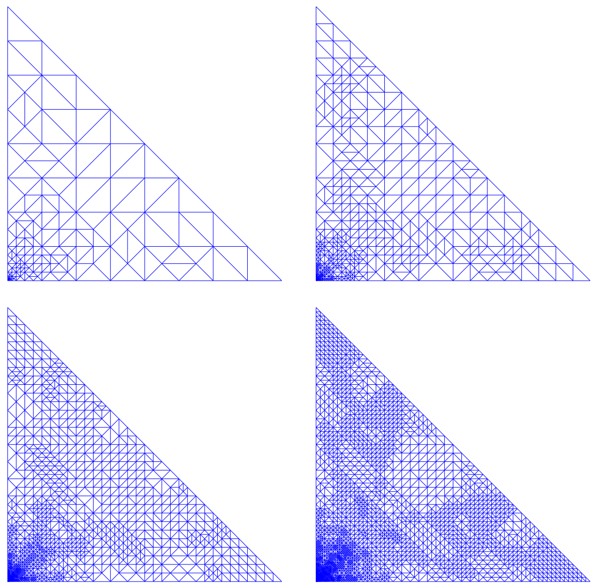

Figure 2: Adaptive refined meshes corresponding to 983, 3979, 11307 and 24639 dof (from left to right, top - bottom) (Example 7.1, with $\mu = 1.0$)

uniform refinement is applied, the total error behaves as $\mathcal{O}(h^{\lambda})$. Since the exact solution is non smooth enough, this behaviour is in agreement with Theorem 5. On the other hand, from Table 2 we can also notice that the quality of approximation is improved, when performing the adaptive refinement Algorithm 1, based on our a posteriori error estimator η. Indeed, we recover the optimal rate of convergence, as it can be seen in Figure 3 (in log-log scale).

In addition, the proposed adaptive refinement procedure is able to detect the singularity of $\boldsymbol{u}$ and p at origin. This is shown in Figure 4, which contains some of the adapted meshes generated in this process. Concerning the index of efficiency, we observe that their values remain bounded, when considering uniformly refined meshes and the sequence of meshes obtained by applying the proposed adaptive refinement procedure. These let us to state that our a posteriori error estimator η, is reliable and gives us numerical evidence of its efficiency.

7.3 The lid-driven cavity problem

Here, we consider problem (1), with $\Omega := (0,1)^2$, $\mu = 1.0$ and $\boldsymbol{f} = \mathbf{0}$. The displacement $\boldsymbol{g}$ on $\partial\Omega$ is defined such that $\boldsymbol{g} = (0,1)^{\mathtt{t}}$ on $\{0\} \times (0,1)$ and $\boldsymbol{g} = \mathbf{0}$ on $\partial\Omega \backslash \{0\} \times (0,1)$. We notice that in this case, $\boldsymbol{g}$ belongs to $[L^2(\Gamma)]^2$ but not to $[H^{1/2}(\Gamma)]^2$. Moreover, we know that the exact solution of (1), $(\boldsymbol{u}, p)$ lives in $[L^2(\Omega)]^2 \times H^{-1}(\Omega)/\mathbb{R}$. As a consequence, the *stress* $\boldsymbol{\sigma} \in [H^{-1}(\Omega)]^{2\times 2}$, and then (15) is not an appropriate mixed formulation for seeking $(\boldsymbol{\sigma}, \boldsymbol{u})$. Then, we point out that this problem is not covered by our a priori error estimate (cf. Theorem 5), due to the lack of regularity. However, the proposed adaptive refinement Algorithm 1, based on our a posteriori error estimator

dof	$\boldsymbol{e}(\boldsymbol{u})$	$r(\boldsymbol{u})$	$\boldsymbol{e}(\boldsymbol{\sigma})$	$r(\boldsymbol{\sigma})$	$\boldsymbol{e}$	r	$\boldsymbol{e}/\eta$
855	0.125e+1	-0.0000	0.249e+1	-0.0000	0.279e+1	-0.0000	1.0247
3275	0.860e+0	0.5632	0.176e+1	0.5192	0.195e+1	0.5279	1.0262
12819	0.587e+0	0.5604	0.123e+1	0.5199	0.136e+1	0.5275	1.0236
50723	0.402e+0	0.5513	0.859e+0	0.5224	0.949e+0	0.5277	1.0206
201795	0.276e+0	0.5454	0.599e+0	0.5238	0.659e+0	0.5276	1.0172
dof	$\boldsymbol{e}(\boldsymbol{u})$	$r(\boldsymbol{u})$	$\boldsymbol{e}(\boldsymbol{\sigma})$	$r(\boldsymbol{\sigma})$	$\boldsymbol{e}$	r	$\boldsymbol{e}/\eta$
855	0.125e+1	-0.0000	0.249e+1	-0.0000	0.279e+1	-0.0000	1.0247
945	0.107e+1	3.2359	0.224e+1	2.1062	0.248e+1	2.3254	1.0267
1327	0.946e+0	0.7106	0.192e+1	0.9017	0.214e+1	0.8654	1.0369
1481	0.818e+0	2.6585	0.172e+1	2.0055	0.190e+1	2.1293	1.0075
2165	0.707e+0	0.7665	0.154e+1	0.5966	0.169e+1	0.6271	1.0325
3357	0.577e+0	0.9296	0.130e+1	0.7652	0.142e+1	0.7931	1.0102
5311	0.477e+0	0.8233	0.110e+1	0.7379	0.120e+1	0.7517	0.9918
8213	0.402e+0	0.7927	0.920e+0	0.8036	0.100e+1	0.8019	1.0125
12323	0.348e+0	0.7047	0.786e+0	0.7776	0.860e+0	0.7658	1.0175
18279	0.283e+0	1.0420	0.658e+0	0.9057	0.716e+0	0.9275	1.0126
27909	0.233e+0	0.9214	0.540e+0	0.9279	0.589e+0	0.9269	1.0057
40595	0.198e+0	0.8765	0.459e+0	0.8761	0.499e+0	0.8762	1.0100
60301	0.165e+0	0.9343	0.379e+0	0.9684	0.413e+0	0.9630	1.0081
91139	0.133e+0	1.0240	0.311e+0	0.9463	0.339e+0	0.9585	1.0081
132705	0.112e+0	0.9087	0.258e+0	1.0076	0.281e+0	0.9921	1.0027

Table 2: History of convergence and corresponding rates of convergence, Example 7.2, with $\mu = 1.0$ (uniform and adaptive refinements)

(cf. (38)), is robust enough to identify the singularities at $(0,0)$ and $(0,1)$. The directional field of displacement $\boldsymbol{u}_h$ is displayed in Figure 5 (left). The isovalues of the post-processed hydrostatic pressure $p_h := -\frac{1}{2}\mathrm{tr}(\boldsymbol{\sigma}_h)$ (with no oscillations), at an intermediate mesh, generated by performing the adaptive refinement algorithm, are shown in Figure 5 (right) . The numerical results give us experimental evidence that the set of local a posteriori error estimators $\{\eta_T\}_{T\in\mathcal{T}_h}$ helps the adaptive refinement algorithm, to recognize the singularities of the *stress* and the displacement in the adapted meshes.

Concluding remarks

In this article we have introduced a new stabilized scheme for the equations describing the incompressible elasticity phenomena, approximated by an stress-displacement formulation. In this framework, usually the symmetry of the stress tensor is imposed by introducing the rotation as a new unknown. In order to circumvent this additional unknown, we partially follow [20] (see also [8]), and we proceed by defining a skew symmetric tensor of the gradient of the displacement. Then, in order to extend the possibility of using more elements, the scheme is stabilized by augmenting it with residual terms. The resulting formulation results to be coercive. Therefore, existence, uniqueness, stability and optimal

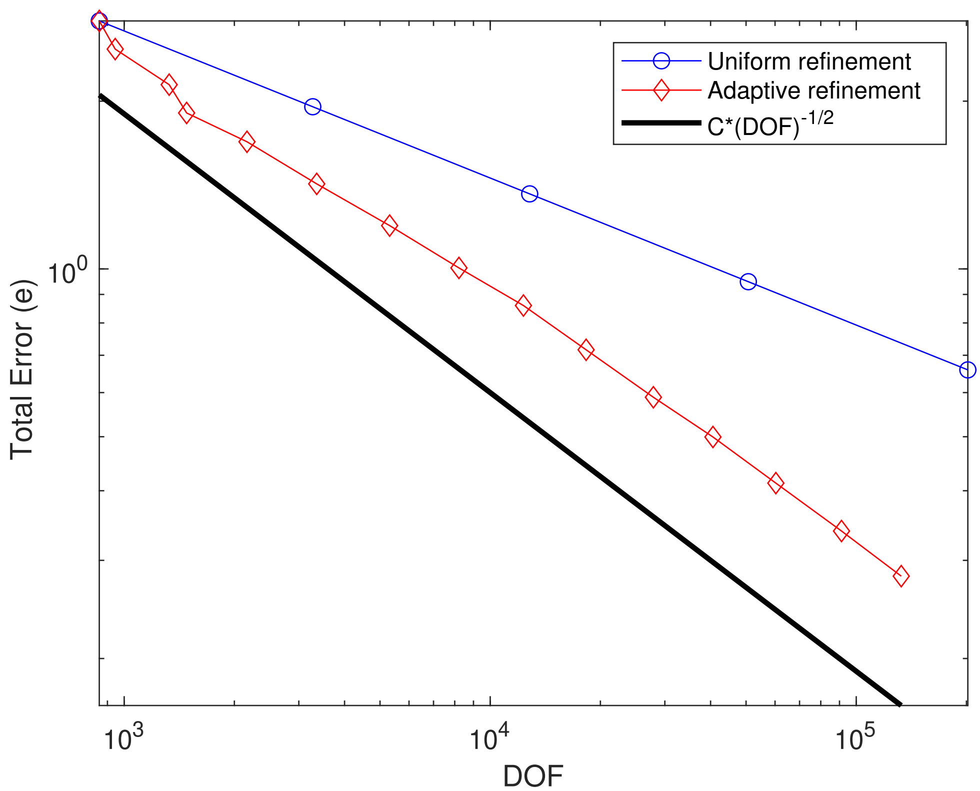

Figure 3: Total error ($\boldsymbol{e}$) vs DOF (N) for uniform and adaptive refinements (Example 7.2, with $\mu = 1.0$)

convergence are guaranteed. Additionally, we provide the scheme with an a-posteriori error estimator, which is reliable and local efficient. In this work we analyze first the problem with pure Dirichlet condition. After that, we extend the approach to deal with mixed boundary conditions. Indeed, the current analysis is also valid for 3D. In this case, we just need to take into account that $p = \frac{1}{3}\,\mathrm{tr}(\boldsymbol{\sigma})$ and $\boldsymbol{\sigma}^{\mathrm{d}} := \boldsymbol{\sigma} - \frac{1}{3}\,\mathrm{tr}(\boldsymbol{\sigma})\,\boldsymbol{I}$, with $\boldsymbol{I}$ denoting the identity tensor or order three.

The numerical examples are developed using the lowest pair, that is, using the lowest order of Raviart-Thomas element for each row of the stress tensor, and continuous piecewise polynomial of degree one for the displacement. In all of them, we can see the optimal convergence of the scheme, as well as its robustness to approximate problems with low regularity. Moreover, we emphasize that the scheme works correctly for example provided in Section 7.3, which is not covered by the current analysis. As a complementary information of this topic, we remark that in [27] the authors deal with the Stokes problem with non smooth Dirichlet datum $\boldsymbol{g}$. The key strategy relies on considering a suitable approximation $\boldsymbol{g}_h$ of $\boldsymbol{g}$, in order to compute an approximation of the solution.

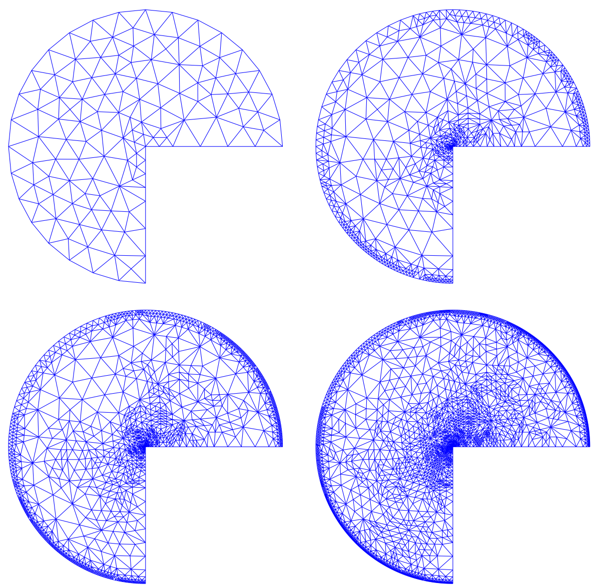

Figure 4: Adaptive refined meshes corresponding to 945, 5311, 12323 and 27909 dof (from left to right, top - bottom) (Example 7.2, with $\mu = 1.0$)

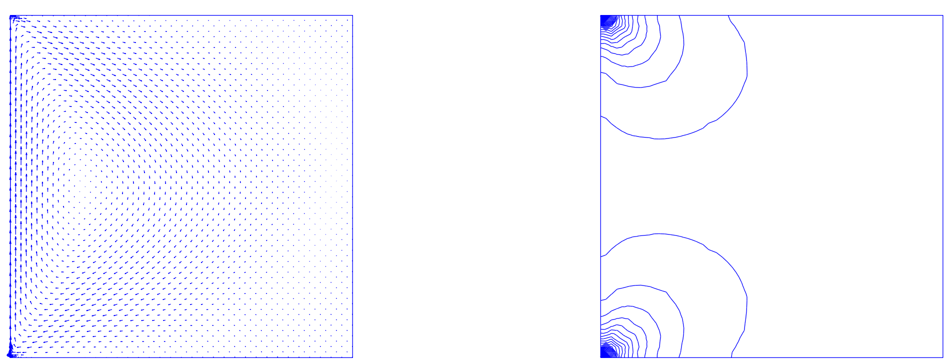

Figure 5: Directional field of displacement $\boldsymbol{u}_h$ (left) and isovalues of hydrostatic pressure p_h (right), corresponding to an intermediate adapted mesh with 17831 dof (Example 7.3 with $\mu = 1.0$)

Acknowledgments. The authors have been partially supported by ANID-Chile through FONDECYT grant 1200051. Tomás P. Barrios and Edwin M. Behrens have been partially supported by Dirección de Investigación of Universidad Católica de la Santísima Concepción (Chile), through Incentivo Mensual program. All authors have contributed equally in this article.

References

[1] D. N. Arnold, F. Brezzi and J. Douglas, Jr., *PEERS: a new mixed finite element for plane elasticity.* Japan Journal of Applied Mathematics, vol. 1, pp. 347–367, (1984).

[2] D. N. Arnold, F. Brezzi and Ch. P. Gupta, *A family of higher order mixed finite element methods for plane elasticity.* Numerische Mathematik, vol. 45, pp. 1–22, (1984).

[3] M. Barrientos, G. N. Gatica, E. P. Stephan, *A mixed finite element method for nonlinear elasticity: two-fold saddle point approach and a-posteriori error estimate.* Numerische Mathematik, vol. 91 (2), pp. 197–222, (2002).

[4] T. P. Barrios, E. M. Behrens and R. Bustinza, *A stabilised mixed method applied to Stokes system with nonhomogeneous source terms: The stationary case.* International Journal for Numerical Methods in Fluids, vol. 92, pp. 509–527, (2020).

[5] T. P. Barrios, E. M. Behrens and R. Bustinza, *An a posteriori error estimate for a dual mixed method applied to Stokes system with non null source terms.* Advances in Computational Mathematics (to appear).

[6] T.P. Barrios, E. M. Behrens and M. González, *A posteriori error analysis of an augmented mixed formulation in linear elasticity with mixed and Dirichlet boundary conditions.* Computer Methods Applied Mechanics and Engineering, vol. 200, pp. 101–113, (2011).

[7] T. P. Barrios, E. M. Behrens and M. González, *Low cost A posteriori error estimators for an augmented mixed FEM in linear elasticity.* Applied Numerical Mathematics, vol. 84, pp. 46–65, (2014).

[8] T. P. Barrios, E. M. Behrens and M. González, *New a posteriori error estimator for an stabilized mixed method applied to incompressible fluid flows.* Applied Mathematics and Computation, vol. 351, pp. 37–47, (2019).

[9] T. P. Barrios, E. M. Behrens and M. González, *A posteriori error analysis of an augmented dual-mixed method in linear elasticity with mixed boundary conditions.* International Journal of Numerical Analysis and Modeling, vol. 16, pp. 804–824, (2019).

[10] T. P. Barrios, R. Bustinza, G.C. García and M. González, *An a posteriori error analysis of a velocity-stress formulation of the generalized Stokes problem.* Journal of Computational and Applied Mathematics, vol. 357, 349–365, (2019).

[11] T. P. Barrios, R. Bustinza, G. García and M. González, *An a posteriori error estimator for a new stabilized formulation of the Brinkman problem.* Numerical Mathematics and Advanced Applications - ENUMATH-2013, 10^{th} European Conference on Numerical Mathematics and Advanced Applications, Lausanne, August 2013. Abdulle, A., Deparis, S., Kressner, D., Nobile, F., Picasso, M. (Editors), LNCSE, vol. 103, pp. 263 – 271. Springer Verlag, 2015.

[12] T.P. Barrios, R. Bustinza, G. C. García, and E. Hernández, *On stabilized mixed methods for generalized Stokes problem based on the velocity-stress formulation: A priori error estimates.* Computer Methods in Applied Mechanics and Engineering, vol. 237-240, pp. 78–87, (2012).

[13] T. P. Barrios, J. M. Cascón and M. González, *A posteriori error analysis of a stabilized mixed finite element method for Darcy flow.* Computer Methods in Applied Mechanics and Engineering, vol. 283, pp. 909–922, (2015).

[14] T. P. Barrios, J. M. Cascón and M. González, *A posteriori error estimation of a stabilized mixed finite element method for Darcy flow.* In book: Proceedings of International conference Boundary and Interior Layers - Computational & Asymptotic Methods, BAIL 2014 (Edited by Petr Knobloch). Springer series Lecture Notes in Computational Science and Engineering, vol. 108, pp. 13 – 23. (2015).

[15] T. P. Barrios, J. M. Cascón and M. González, *Augmented mixed finite element method for the Oseen problem: A priori and a posteriori error analysis.* Computer Methods in Applied Mechanics and Engineering, vol. 313, pp. 216–238, (2017).

[16] T.P. Barrios and G.N. Gatica, *An augmented mixed finite element method with Lagrange multipliers: A priori and a posteriori error analyses.* Journal of Computational and Applied Mathematics, vol. 200, pp. 653–676, (2007).

[17] T.P. Barrios, G.N. Gatica, M. González and N. Heuer, *A residual based a posteriori error estimator for an augmented mixed finite element method in linear elasticity.* M2AN Mathematical Modelling and Numerical Analysis, vol. 40, pp. 843–869, (2006).

[18] D. Braess, Finite Elements. Cambridge University Press, Third Edition, Cambridge, 2007.

[19] F. Brezzi and M. Fortin, Mixed and hybrid finite element methods. Springer Series in Computational Mathematics 15, Springer-Verlag, New York, 1991.

[20] J. Camaño, R. Oyarzúa, R. Ruiz-Baier and G. Tierra, *Error analysis of an augmented mixed method for the Navier-Stokes problem with mixed boundary conditions.* IMA Journal of Numerical Analysis, vol. 38, pp. 1452–1484 , (2018).

[21] C. Carstensen and G. Dolzmann, *A posteriori error estimates for mixed FEM in elasticity.* Numerische Mathematik, vol. 81, pp. 187–209, (1998).

[22] J. M. Cascón, R. H. Nochetto and K. G. Siebert, *Design and Convergence of AFEM in H(DIV)*, Mathematical Models and Methods in Applied Sciences. vol. 17 (11), pp. 1849 – 1881 , (2007).

[23] M. Chiumenti, Q. Valverde, C. Agelet de Saracibar and M. Cervera, *A stabilized formulation for incompressible elasticity using linear displacement and pressure interpolations*, Computer Methods in Applied Mechanics and Engineering, vol. 191 (46), pp. 5253–5264, (2002).

[24] P.G. Ciarlet, The Finite Element Method for Elliptic Problems. North-Holland, 1978.

[25] P. Clément, *Approximation by finite element functions using local regularisation.* RAIRO Modélisation Mathématique et Analyse Numérique, vol. 9, pp. 77–84, (1975).

[26] S. Du and F.-J. Sayas, An invitation to the Theory of the Hybridizable Discontinuous Galerkin Method. SpringerBriefs in Mathematics, Springer Nature, Switzerland AG, 2019.

[27] R. Durán, L. Gastaldi and A.L. Lombardi, *Analysis of finite element approximations of Stokes equations with non-smooth data.* SIAM Journal of Numerical Analysis, vol. 58, 6, pp. 3309–3331, (2020).

[28] A. Ern and J.L. Guermond, Theory and Practice of Finite Elements, Springer-Verlag, New York, 2004.

[29] L. Figueroa, G. N. Gatica and N. Heuer, *A priori and a posteriori error analysis of an augmented mixed finite element method for incompressible fluid flows.* Computer Methods in Applied Mechanics and Engineering, vol. 198, 2, pp. 280–291, (2008).

[30] L. Figueroa, G. N. Gatica and A. Márquez, *Augmented mixed finite element methods for the stationary Stokes equations.* SIAM Journal on Scientific Computing, vol. 31, 2, pp. 1082–1119, (2008).

[31] G.N. Gatica, *Analysis of a new augmented mixed finite element method for linear elasticity allowing* $\mathbb{RT}_0$-$\mathbb{P}_1$-$\mathbb{P}_0$ *approximations.* M2AN Mathematical Modelling and Numerical Analysis, vol. 40, pp. 1–28, (2006).

[32] G.N. Gatica, *An augmented mixed finite element method for linear elasticity with non-homogeneous Dirichlet conditions.* Electronic Transactions on Numerical Analysis, vol. 26, pp. 421–438, (2007).

[33] R. Hiptmair, *Finite elements in computational electromagnetism.* Acta Numerica, vol. 11, pp. 237–339, (2002).

[34] J.E. Roberts and J.-M. Thomas, *Mixed and Hybrid Methods.* In: Handbook of Numerical Analysis, edited by P.G. Ciarlet and J.L. Lions, vol. II, Finite Element Methods (Part 1), 1991, North-Holland, Amsterdam.

[35] R. Verfürth, *A posteriori error estimation and adaptive mesh-refinement techniques*, Journal of Computational and Applied Mathematics, vol. 50, pp. 67–83, (1994).

[36] R. Verfürth, A Review of a Posteriori Error Estimation and Adaptive Mesh-Refinement Techniques, Wiley-Teubner, Chichester, 1996.

[37] R. Verfürth, *A Review of A Posteriori Error Estimation Techniques for Elasticity Problems.* Computer Methods in Applied Mechanics and Engineering, vol. 176, 1, pp. 419–440, (1999).

Centro de Investigación en Ingeniería Matemática (CI^{2}MA)

PRE-PUBLICACIONES 2021

2021-15 Raimund Bürger, Julio Careaga, Stefan Diehl, Romel Pineda: *A moving-boundary model of reactive settling in wastewater treatment*

2021-16 Sergio Caucao, Gabriel N. Gatica, Juan P. Ortega: *A fully-mixed formulation in Banach spaces for the coupling of the steady Brinkman–Forchheimer and double-diffusion equations*

2021-17 David Mora, Alberth Silgado: *A C1 virtual element method for the stationary quasi-geostrophic equations of the ocean*

2021-18 Alfredo Bermúdez, Bibiana López-Rodríguez, Francisco José Pena, Rodolfo Rodríguez, Pilar Salgado, Pablo Venegas: *Numerical solution of an axisymmetric eddy current model with current and voltage excitations*

2021-19 Raimund Bürger, Sonia Valbuena, Carlos A. Vega: *A well-balanced and entropy stable scheme for a reduced blood flow model*

2021-20 Gabriel N. Gatica, Cristian Inzunza, Ricardo Ruiz-Baier, Felipe Sandoval: *A posteriori error analysis of Banach spaces-based fully-mixed finite element methods for Boussinesq-type models*

2021-21 David Mora, Iván Velásquez: *A C^1-C^0 conforming virtual element discretization for the transmission eigenvalue problem*

2021-22 Ricardo Oyarzúa, Manuel Solano, Paulo Zuñiga: *Analysis of an unfitted mixed finite element method for a class of quasi-Newtonian Stokes flow*

2021-23 Felisia A. Chiarello, Harold D. Contreras, Luis M. Villada: *Nonlocal reaction traffic flow model with on-off ramps*

2021-24 Sergio Caucao, Ricardo Oyarzúa, Segundo Villa-Fuentes, Ivan Yotov: *A three-field Banach spaces-based mixed formulation for the unsteady Brinkman-Forchheimer equations*

2021-25 Reinaldo Campos-Vargas, Esther Carrera, Bruno G. Defilippi, Claudia Fuentealba, Ignacia Hernández, Maarten Hertog, Claudio Meneses, Gerardo Nuñez, Diego Paredes, Romina Pedreschi, Virgilio Uarrota: *Transcriptome and hormone analyses reveals differences in physiological age of “Hass” avocado fruit*

2021-26 Tomás Barrios, Edwin Behrens, Rommel Bustinza: *Numerical analysis of a stabilized mixed method applied to incompressible elasticity problems with Dirichlet and with mixed boundary conditions*

Para obtener copias de las Pre-Publicaciones, escribir o llamar a: Director, Centro de Investigación en Ingeniería Matemática, Universidad de Concepción, Casilla 160-C, Concepción, Chile, Tel.: 41-2661324, o bien, visitar la página web del centro: `http://www.ci2ma.udec.cl`




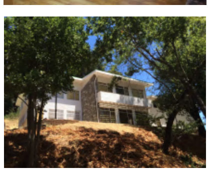

CENTRO DE INVESTIGACIÓN EN
INGENIERÍA MATEMÁTICA (CI^{2}MA)
Universidad de Concepción

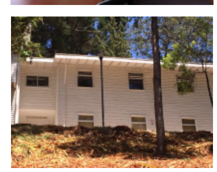
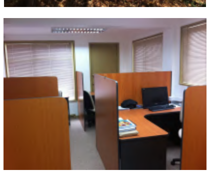

Casilla 160-C, Concepción, Chile
Tel.: 56-41-2661324/2661554/2661316
http://www.ci2ma.udec.cl